



# Estimating ancestral ranges and biogeographical processes in early hominins



Yeganeh Sekhavati <sup>a,\*</sup>, David Strait <sup>a,b</sup>

<sup>a</sup> Department of Anthropology, Washington University in St. Louis, St. Louis, MO 63130, USA

<sup>b</sup> Palaeo-Research Institute, University of Johannesburg, Cnr Kingsway and University Road Auckland Park, PO Box 524, Auckland Park 2006, South Africa

## ARTICLE INFO

### Article history:

Received 1 December 2022

Accepted 6 May 2024

### Keywords:

Australopith

*Homo*

Vicariance

Dispersal

Sympatry

## ABSTRACT

Historical biogeography provides crucial insights into understanding the evolutionary history of hominins. We applied maximum-likelihood and biogeographical stochastic mapping to infer the ancestral ranges of hominins and estimate the frequency of biogeographical events. These events were inferred using two time-calibrated phylogenetic trees that differ in the position of *Australopithecus sediba*. Results suggest that regardless of which phylogeny was selected, Northcentral Africa was the preferred ancestral region for the ancestor of the *Homo-Pan* clade, as well as the ancestor of *Sahelanthropus* and later hominins. The northern and middle part of eastern Africa was the preferred ancestral region for several clades originating at subsequent deep nodes of the trees (~5–4 Ma). The choice of tree topology had one important effect on results: whether hominin ancestors appearing after ~4 Ma were widespread or endemic. These different patterns highlight the biogeographic significance of the phylogenetic relationships of *A. sediba*. Overall, the results showed that dispersal, local extinction, and sympatry played vital roles in creating the hominin distribution, whereas vicariance and jump dispersal were not as common. The results suggested symmetry in the directionality of dispersals. Distance probably influenced how rapidly taxa colonized a new region, and dispersals often followed the closest path. These findings are potentially impacted by the imperfection of the fossil record, suggesting that the results should be interpreted cautiously.

© 2024 Elsevier Ltd. All rights are reserved, including those for text and data mining, AI training, and similar technologies.

## 1. Introduction

### 1.1. General background

Biogeographical analyses are critical to understanding hominin evolutionary history, and the importance of biogeographic processes has been discussed in the paleoanthropological literature for decades. Dispersal, in particular, has been a central focus of many studies. For example, researchers have discussed the importance of dispersals in hominin diversification (e.g., Lahr and Foley, 1994; Foley, 2003, 2013), environmental and spatial factors affecting hominin dispersal (e.g., Bromage and Schrenk, 1995; Cuthbert et al., 2017; Foley, 2018; Joordens et al., 2019; Mondanaro et al., 2020), and dispersals in contemporaneous fauna (e.g., Turner and Wood, 1993; Dennell et al., 2014; Carotenuto et al., 2016). Some

researchers pointed to vicariance (e.g., Vrba, 1992; Trauth et al., 2010) and other biogeographic processes (e.g., sympathy; see below) as being critical in hominin evolution (e.g., Schroer and Wood, 2015; Haile-Selassie et al., 2016; Macho, 2017).

Previous phylogeny-based studies of hominin biogeography used maximum parsimony to infer dispersal events (Strait and Wood, 1999; Strait, 2013). Strait and Wood (1999) were the first to analyze hominin biogeography in a phylogenetic framework. They treated geography as a cladistic character in which geographical regions were considered distinct character states. They inferred the evolution of the geography character implied by several cladograms (Delson, 1986; Walker et al., 1986; Grine, 1988; Skelton and McHenry, 1992; Wood, 1992; Strait et al., 1997) by estimating the ancestral areas at the internal nodes of the trees. According to the parsimony criterion, the optimal ancestral distributions minimize the number of character state changes, and any change in character state was a posteriori interpreted as a dispersal event. Strait and Wood (1999) observed four to seven dispersals between southern, eastern, and South-central Africa. More

\* Corresponding author.

E-mail address: [ysekhavati@wustl.edu](mailto:ysekhavati@wustl.edu) (Y. Sekhavati).

recently, [Strait \(2013\)](#) used a similar method to suggest that the last common ancestor (LCA) of hominins originated in central Africa and that significant evolutionary events such as postcanine megadontia and increases in brain size took place in eastern Africa.

[Strait and Grine's \(2004\)](#) and [Strait's \(2013\)](#) prior work provides a useful set of hypotheses for testing. Their findings suggest that early human evolution in Africa involved four specific dispersal events. The first dispersal involved the LCA of hominins, except *Sahelanthropus*, which moved from central to eastern Africa before 6.0 Ma. The second dispersal involved *Australopithecus africanus* or its ancestor moving from eastern to southern Africa before 3.0 Ma. The third dispersal involved *Paranthropus robustus* or its ancestor moving from eastern to southern Africa before 1.8 Ma. Finally, *Homo habilis* dispersed from eastern to southern Africa before 1.8 Ma in the fourth dispersal event.

Since then, additional hominin species have been discovered, and our knowledge of their locations and temporal range have improved (e.g., [Berger et al., 2010](#); [Clarke and Kuman, 2019](#); [Herries et al., 2020](#)). Moreover, while previous studies have used phylogenetic data to estimate the importance and directionality of dispersal events in human evolution (e.g., [Strait and Wood, 1999](#); [Strait, 2013](#)), other biogeographical processes during human evolutionary history require consideration. The objective of this study is to (1) evaluate [Strait's \(2013\)](#) hypotheses concerning the most likely ancestral range distribution of early hominin taxa, as well as the directionality of dispersals, (2) estimate the biogeographic processes that underlie species distributions (see below), and (3) assess the frequency of biogeographic events by examining alternative biogeographic scenarios.

## 1.2. Recent developments in historical biogeography

As noted, phylogeny-based reconstructions of biogeography have relied on parsimony. Parsimony-based reconstructions of hominin biogeography have several shortcomings. These methods have been applied to find dispersal patterns, but dispersal is only one of many biogeographical processes ([Ronquist, 1995](#); [Ronquist and Sanmartín, 2011](#)). Moreover, although dispersal can explain any distribution pattern, these hypotheses are not subject to falsification ([Morrone and Crisci, 1995](#); [Sanmartín and Ronquist, 2004](#)). For these reasons, [Ronquist \(1995\)](#) referred to these methods as 'pattern-based,' which determine evolutionary processes after the results have been obtained (for more information, see [Ronquist and Sanmartín, 2011](#)). Additionally, parsimony ignores critical information about time (i.e., branch length). Therefore, longer branch lengths do not have an associated higher probability of change. Finally, the parsimony method used in previous studies ([Strait and Wood, 1999](#); [Strait, 2013](#)) assumes that ancestors occur in single areas. However, such an assumption does not reflect widespread hominin taxa discovered from multiple sites. The problem with reconstructing single-area ancestors is that, to invoke vicariance, we need to be able to infer widespread ancestors at the nodes that divide into smaller regions ([Lamm and Redelings, 2009](#); [Crisp et al., 2011a, 2011b](#)).

In recent years, historical biogeography has been transformed significantly through the development of statistical approaches and 'event-based' methods ([Ronquist, 1997](#); [Ree et al., 2005](#); [Landis et al., 2013](#); [Matzke, 2013](#); [Ree and Sanmartín, 2018](#)). These methods estimate geographic range evolution along branches of phylogenetic trees (i.e., anagenetic events) and at internal nodes of the tree (i.e., cladogenetic events; [Matzke, 2013](#)). The methodological transition was initiated by dispersal-vicariance analysis (DIVA) in the 1990s ([Ronquist, 1997](#)). Dispersal-vicariance analysis is an 'event-based' parsimony method that estimates ancestral distribution and biogeographical processes. The two types of

anagenetic events allowed in DIVA ([Fig. 1](#)) are dispersal and local extinction (see above). Cladogenetic events that are allowed ([Fig. 1](#)) are narrow sympatry, as well as narrow and widespread vicariance. Dispersal-vicariance analysis uses a three-dimensional cost matrix that counts biogeographical events ([Ronquist, 1997](#)). It assigns a cost of one for extinction and dispersal events, whereas vicariance and duplication within a single area (i.e., narrow sympatry) have zero costs ([Ronquist, 1997](#); for more information, see [Sanmartín and Ronquist, 2004](#)). The most parsimonious solution is the estimation that explains the data with the least cost. As a result, DIVA favors hypotheses that minimizes the number of dispersal events.

A maximum likelihood approach to infer geographic range evolution was first proposed by [Ree et al. \(2005\)](#) and was later refined by [Ree and Smith \(2008\)](#). This approach, dispersal–extinction–cladogenesis (DEC) is a parametric model that assigns probabilities, rather than costs, to events. Anagenetic events (i.e., dispersal and extinction) are free parameters used to create an instantaneous rate matrix (i.e., a matrix describing transition rates between discrete geographic ranges along phylogenetic branches). Next, the likelihood of alternative range inheritance scenarios at the cladogenesis events is calculated. Regarding cladogenetic events, both DIVA and DEC allow narrow sympatry and narrow vicariance but disallow widespread sympatry ([Fig. 1](#)). However, the two models differ concerning two cladogenetic processes. First, DIVA allows widespread vicariance (see previous text), whereas DEC assumes that one of the daughters must always have a range of only one area. As a result, widespread vicariance is not allowed in DEC. Second, unlike DIVA, DEC allows subset sympatry ([Ronquist and Sanmartín, 2011](#)).

One of the shortcomings of the DEC model is its computational limit as the number of areas increases. A Bayesian approach called Bayesian inference of historical biogeography for discrete areas (BayArea; [Landis et al., 2013](#)) enhances the computational speed of biogeographic models while enabling biogeographic inference at a finer scale. In BayArea, ancestral ranges are assumed to be identical at cladogenesis events. Consequently, this model allows only widespread and narrow sympatry (see previous text) at cladogenetic events ([Fig. 1](#)), where two daughter lineages inherit the same range(s) as their ancestor. Widespread sympatry is only allowed in BayArea and is prohibited in DIVA and DEC models. Here, we use the new approaches to test biogeographic hypotheses and model biogeographic processes in early hominins.

## 2. Materials and methods

### 2.1. Taxonomy

[Martin et al. \(2024\)](#) have recently revised hominin taxonomy based on first principles of species concept theory. Following [de Querioz \(1998, 2007\)](#), they note that species are segments of lineages representing ancestor and descendant metapopulations that have diverged from (and are thus largely independent of) other such segments, originating at a point of lineage divergence and extending until either extinction or a subsequent divergence point. This ontological definition is known ([de Querioz, 2007](#)) as the unified species concept (USC). Most other species concepts are epistemological attempts to approximate this species ontology. Conventionally, hominin species are defined (either implicitly or explicitly) using the phylogenetic species concept (PSC), which operationally defines species as clusters of organisms that are diagnosably distinct from other such groups (in the context of hominin species, diagnosability generally reflects morphological distinctiveness). A problem with the PSC is that the morphological diagnosability needs not necessarily evolve at the very base of a lineage segment, meaning that early and late populations of a single lineage segment could be diagnosably distinct from each

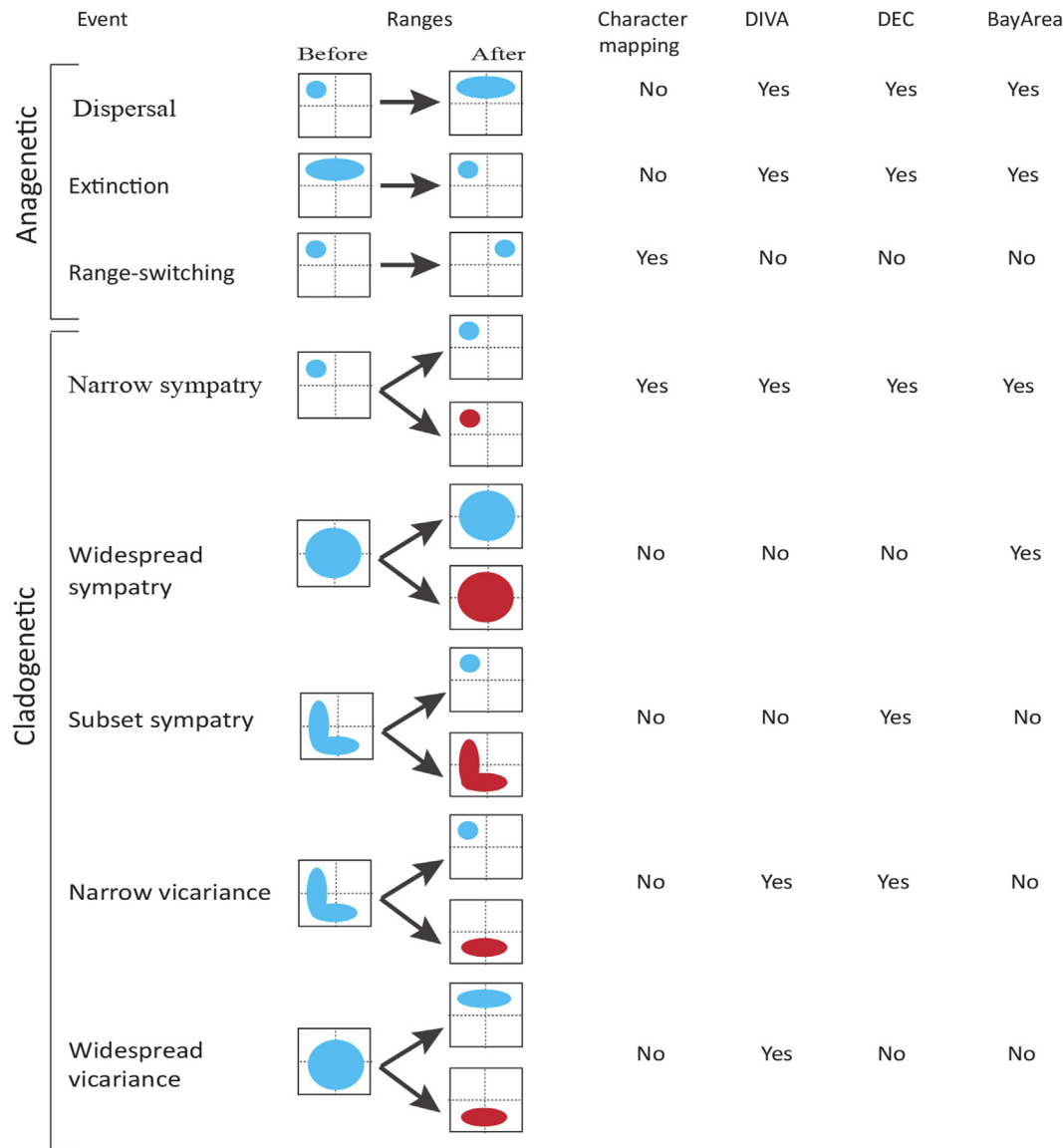


**Figure 1.** Biogeographic processes assumed by each method. Anagenetic events occur along branches of phylogenetic trees, and cladogenetic events at internal nodes of the tree. Adapted from Matzke (2013). Abbreviations: DIVA = dispersal–vicariance analysis; DEC = dispersal–extinction–cladogenesis model; BayArea = Bayesian inference of historical biogeography for many discrete areas.

other and thus would be misclassified as different species. Martin et al. (2024) propose instead that distinct species should be recognized only when lineage divergence can be demonstrated (thereby falsifying a single species null hypothesis), and that such a demonstration can be achieved by considering both morphology and chronology (i.e., lineage divergence has occurred when contemporaneous fossil assemblages are diagnosably distinct from each other). Applying the principles of the USC to paleoanthropology means that much fewer species are recognized (Martin et al., 2024) and that several taxa previously identified as species should be reduced in rank to subspecies. Thus, both the PSC and USC allow recognition of many of the same taxa, but several of those taxa are placed in different taxonomic categories (Table 1).

From the standpoint of nomenclature, it is very easy to “convert” the taxon names recognized using the PSC to those using the USC (Table 1). However, to do so in this study would be inappropriate; many of the USC taxa are subspecies, and as explained by Martin et al. (2024), species are independent from other equivalent taxa, whereas subspecies are not (i.e., they are nested within species and

thus are not truly independent). In the present study, which was conceived and executed prior to Martin et al. (2024) revised taxonomy, the taxa being analyzed are considered independent units in the phylogenies used to infer biogeographic patterns (see further in the text). As part of those analyses, divergence times are inferred for nodes in the trees that influence branch lengths and, thus, biogeographic patterns. Many of those inferred branching points violate the assumptions of the USC taxa in which several represent early and late populations within a temporally constrained lineage. Thus, the present study should be considered an analysis of hominin biogeography under the assumption that the taxa conventionally recognized using the PSC represent true species. A consideration of biogeography using hominin taxa defined using principles of the USC must await further study.

## 2.2. Hominin phylogeny and species distribution

Ingroup taxa included in this study are *Sahelanthropus tchadensis*, *Ardipithecus ramidus*, *Australopithecus anamensis*, *Australopithecus*

**Table 1**

Hominin taxa conventionally recognized using the phylogenetic species concept and the equivalent taxa recognized using principles of the unified species concept.<sup>a</sup>

PSC taxa	Equivalent USC taxa
<i>Sahelanthropus tchadensis</i>	<i>Ardipithecus ramidus tchadensis</i>
<i>Ardipithecus ramidus</i>	<i>Ardipithecus ramidus ramidus</i>
<i>Australopithecus anamensis</i>	<i>Australopithecus afarensis anamensis</i>
<i>Australopithecus afarensis</i>	<i>Australopithecus afarensis afarensis</i>
<i>Australopithecus garhi</i>	<i>Australopithecus afarensis garhi</i>
<i>Australopithecus africanus</i>	<i>Australopithecus africanus sediba</i>
<i>Paranthropus aethiopicus</i>	<i>Paranthropus boisei aethiopicus</i>
<i>Paranthropus boisei</i>	<i>Paranthropus boisei boisei</i>
<i>Paranthropus robustus</i>	<i>Paranthropus robustus<sup>b</sup></i>
<i>Homo habilis</i>	<i>Homo habilis</i>
<i>Homo rudolfensis</i>	<i>Homo rudolfensis</i>
<i>Homo erectus</i>	<i>Homo erectus</i>

<sup>a</sup> See [Martin et al. \(2024\)](#).

<sup>b</sup> [Martin et al. \(2024\)](#) recognize two subspecies of *Paranthropus robustus*, *Paranthropus robustus robustus* and *Paranthropus robustus ukusa*. The phylogenies on which the present biogeographic analyses are based were published before the latter subspecies was defined, and thus it is not included here but rather is subsumed within a single taxon, *P. robustus*. This should have no effect on the current study because the two subspecies are known from the same geographic region and are time successive. Abbreviations: PSC = phylogenetic species concept; USC = unified species concept.

*afarensis*, *Australopithecus garhi*, *A. africanus*, *Australopithecus sediba*, *Paranthropus aethiopicus*, *P. robustus*, *Paranthropus boisei*, *H. habilis*, *Homo rudolfensis*, and *Homo erectus* s.l. Alpha taxonomy followed [Martin et al. \(2021\)](#) and the phylogenetic analyses to which it is closely allied ([Mongle et al., 2019, 2022, 2023](#); see also [Strait et al., 1997](#); [Strait and Grine, 2004](#)). *Kenyanthropus platyops* was not included in our study because of uncertainty concerning its phylogenetic relationships in the phylogenetic analyses that form the framework of the present study ([Mongle et al., 2019, 2022, 2023](#); [Martin et al., 2021](#); see also [Strait and Grine, 2004](#)).

We used the recent hominin phylogenetic analysis by [Martin et al. \(2021\)](#) as the basis for our tree. To accommodate alternative placements of *A. sediba*, we modified the tree in two ways. First, we considered the placement of *A. sediba* as the sister taxon of *A. africanus*, as suggested by [Irish et al. \(2013\)](#) and [Kimbrel and Rak \(2017\)](#). Second, we also considered the placement of *A. sediba* as the sister taxon of *Homo*, as suggested by [Berger et al. \(2010\)](#). These alternatives are depicted in [Figures 2 and 3](#). For outgroup taxa, we included *Pan troglodytes*, *Pan paniscus*, *Gorilla gorilla*, and *Gorilla beringei*.

*beringei*. Although we explored alternative hypotheses on hominin phylogeny and their effects on the results, the models examined in this study do not consider phylogenetic uncertainty.

Biogeographic regions can be characterized in numerous ways. Defining an exact boundary to differentiate between distinct regions can be fraught, and a certain degree of subjectivity is involved in defining regions. However, there is broad consensus in the literature on historical biogeography that regions should be chosen based on criteria such as co-occurrence of endemic species (e.g., [Morrone, 1994, 2015, 2018](#); [Szumik and Goloboff, 2004](#); [Vilhena and Antonelli, 2015](#); [He et al., 2017](#)), and species turnover ([Kreft and Jetz, 2010](#)). Although such approaches have limitations; they nonetheless have theoretical foundations ([Murguía and Llorente-Bousquet, 2003](#); [Escalante et al., 2013](#)).

We used two methods to define biogeographical regionalization for hominins in Africa. Despite the fact that both methods have limitations and rely on assumptions, those assumptions differ meaningfully. As a consequence, one can have a measure of confidence in any results obtained using both methods.

We first used [Linder et al.'s \(2012\)](#) study on biogeographical regionalization in Sub-Saharan Africa as a coarse guide. [Linder et al. \(2012\)](#) used multiple vertebrates and plant species in Sub-Saharan Africa to define biogeographic regions for the African biota. They identified six primary regions for mammals ([Fig. 4](#)): Saharan, Sudanian, Zambezian, Somalian, a combined Guinean and Congolian region, and the southern Africa region (Kalaharian and South African). Importantly, in their analyses, eastern Africa was not retrieved as only one region and represented a complex biogeographical mixture. Due to the observed complexity in East Africa and incongruent biogeographical signals, [Linder et al. \(2012\)](#) suggested recognizing parts of Congo, Kenya, Uganda, and northcentral Tanzania as a seventh mosaic region. This region is equivalent to an enlarged Lake Victoria region.

[Linder et al.'s \(2012\)](#) biogeographical region are based on comparing the species composition of grid cells using extant taxa. When trying to define areas in the fossil record using modern biogeographic data, there are limitations to consider. These limitations arise because biogeographic regions may have been different in the past due to environmental and climate changes. For example, recent anthropogenic activities have altered species distribution patterns and affected our understanding of macroevolutionary diversity patterns ([Crisci et al., 2006](#); [Faurby and Svenning, 2015](#)). Growing populations, livestock expansion, and land

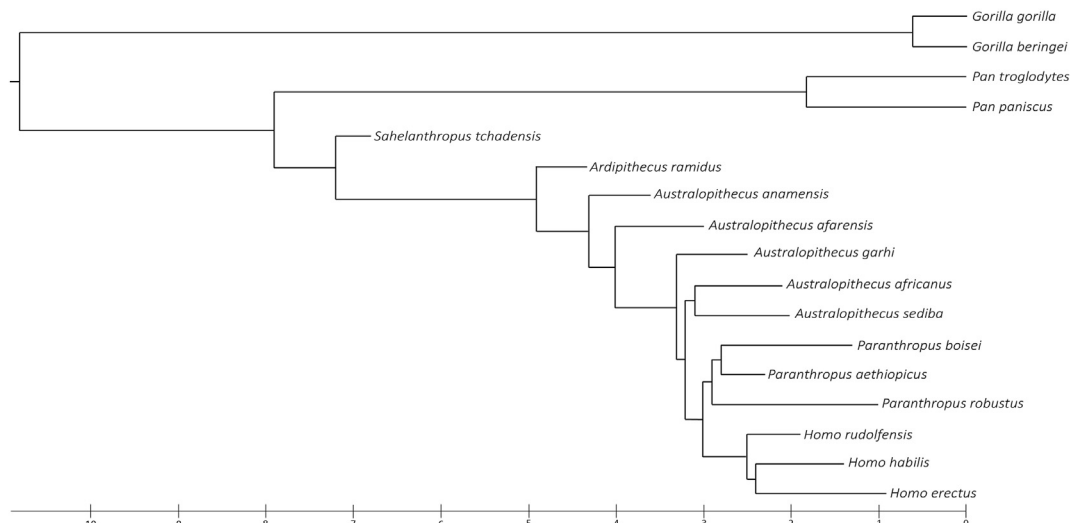


**Figure 2.** Tree 1, modified after [Martin et al. \(2021\)](#). *Australopithecus sediba* is the sister taxon of *Australopithecus africanus* following [Irish et al. \(2013\)](#) and [Kimbrel and Rak \(2017\)](#).

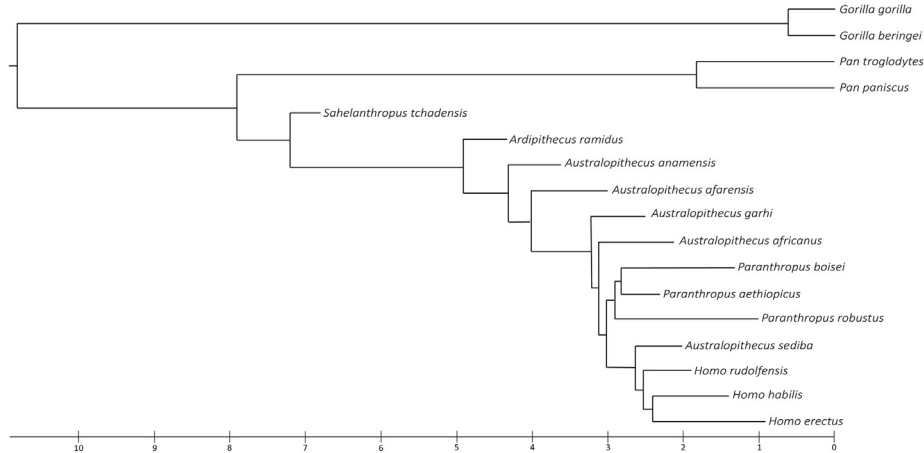


**Figure 3.** Tree 2, modified after [Martin et al. \(2021\)](#). *Australopithecus sediba* is the sister taxon of *Homo*, following [Berger et al. \(2010\)](#).

conversion practices can contribute significantly to landscape changes ([Veldhuis et al., 2019](#); [Boles et al., 2019](#)). This transformative influence is evident in the Serengeti, where the current landscape, dominated by wooded grasslands and short-grass plains, is relatively recent ([Sinclair et al., 2009](#)). Pastoralist communities in the region have played a pivotal role in shaping savanna ecology through establishing settlements, farming, controlled burning, and livestock management practices. Both plant life and large mammals have been affected by these practices ([Vuorio et al., 2014](#)), illustrating the limitations of using contemporary geographical boundaries to analyze past distribution of taxa.

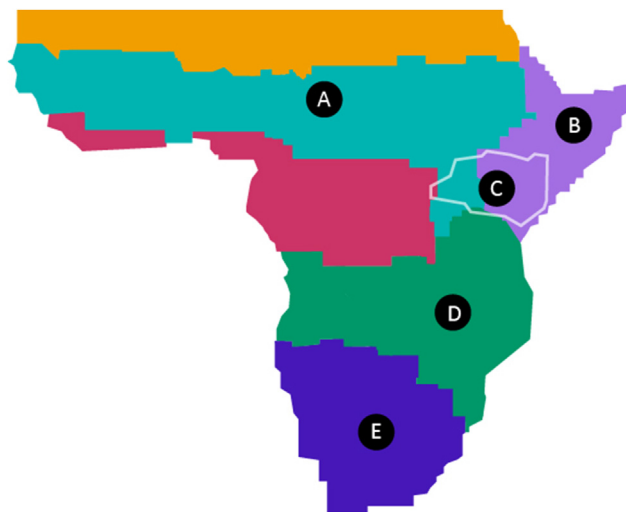


**Figure 4.** Geographic distribution of taxa included in this study. The geographic areas are Northcentral Africa (A), northern part of eastern Africa (B), middle part of eastern Africa (C), southern part of eastern Africa (D), southern Africa (E), central Africa (F). Adapted from [Joordens et al. \(2019\)](#). Taxa distribution: A = *Sahelanthropus tchadensis*, *Australopithecus afarensis*; B = *Ardipithecus ramidus*, *Australopithecus anamensis*, *A. afarensis*, *Australopithecus garhi*, *Homo habilis*, *Homo erectus* s.l.; C = *A. ramidus*, *A. anamensis*, *A. afarensis*, *Paranthropus aethiopicus*, *Paranthropus boisei*, *H. habilis*, *Homo rudolfensis*, *H. erectus* s.l.; D = *P. boisei*, *H. rudolfensis*; E = *A. africanus*, *Australopithecus sediba*, *Paranthropus robustus*, *H. habilis*, *H. erectus* s.l.; F = *Pan* and *Gorilla*. Colors correspond to [Linder et al. \(2012\)](#)'s study of biogeographical regionalization of mammals in sub-Saharan Africa: Orange = Saharan region; light blue = Sudanian region; red = Congolian and Guinean regions; green = Zambezian region; purple = Somalian region; dark blue = southern African region. The white outline marks the mosaic region identified by [Linder et al. \(2012\)](#) (For interpretation of the references to color in this figure legend, the reader is referred to the web version of this article).

Despite these limitations, the method is grounded theoretically in the imperative to identify 'natural areas' and relies on a rich species distribution dataset that cannot be obtained through paleontological data. Therefore, while acknowledging that present biogeographic regions may not accurately represent those of the past, we accept these regions as an approximation of how mammals may have been distributed over geological time. Although we assume that climate oscillations would have caused these regions' boundaries to shift according to fluctuations in temperature and aridity/humidity interacting with variations in topography and atmospheric patterns, we note that [Villaseñor et al. \(2020\)](#) found differences in relative mammalian abundance reflecting paleoecological variation both within and between geological basins preserving hominins in eastern Africa. Thus, the existing paleontological record supports the subdivision of eastern Africa into multiple ecologically diverse regions during at least part of the time period relevant to the present study.

The regions included in our analysis based on [Linder's \(2012\)](#) study are Northcentral Africa (corresponding to the Sudanian region defined by [Linder et al., 2012](#)), northern part of eastern Africa (eastern Africa<sub>North</sub>; corresponding to the Somalian Region), middle part of eastern Africa (eastern Africa<sub>Middle</sub>; corresponding to the mosaic region identified by [Linder et al., 2012](#)), southern part of eastern Africa (eastern Africa<sub>South</sub>; corresponding to the Zambezian Region), southern Africa (corresponding to the southern African region), and central Africa (corresponding to Guinean and Congolian regions). Geographic distribution data of the ingroup and outgroup taxa in this study are provided in [Table 2](#).

We explored an alternative approach by dividing Africa into three smaller biogeographic regions based on [Strait's \(2013\)](#) study: central Africa, eastern Africa, and southern Africa. However, this approach has limitations as it does not consider the biogeographic processes within the expansive eastern African region, where hominins are distributed in a mosaic fashion from north to south ([Fig. 4](#)). Additionally, it conflicts with the findings of [Villaseñor et al. \(2020\)](#) on the ecological complexity in eastern Africa (see above). Moreover, it has been suggested that the number of regions used in biogeography analyses should vary based on the dispersal ability of the studied taxa ([Cox, 2001, 2010](#); [Mateo et al., 2013](#)). Given that hominins are generally thought to have a notable ability to disperse ([Wells and Stock, 2007](#); [Foley, 2013](#)), using a greater number of regions may provide further insights into the dispersal patterns and biogeography of hominins. On the other hand, the method used by [Strait \(2013\)](#) aligns well with the large gaps in our knowledge of the hominin fossil record (potentially influenced by the history of

**Table 2**

Taxa included in this study, their age, and geographic ranges. The geographic regions correspond to those identified by Linder et al. (2012).

Taxon	Region(s)	Age (FAD–LAD, in Ma) <sup>a</sup>
<i>Sahelanthropus tchadensis</i>	A	7.1–6.8 (Lebatard et al., 2008)
<i>Ardipithecus ramidus</i>	B, C	4.8–4.3 (Semaw et al., 2005; Simpson et al., 2019)
<i>Australopithecus anamensis</i>	B, C	4.2–3.6 (Leakey et al., 1995; White et al., 2006; McDougall and Brown, 2008; Haile-Selassie et al., 2010; Brown et al., 2013; Haile-Selassie and Melillo, 2015)
<i>Australopithecus afarensis</i>	A, B, C	3.9–3.0 (Asfaw, 1987; Kimbel et al., 1994; Kimbel and Delezene, 2009; Deino, 2011)
<i>Australopithecus garhi</i>	B	2.5 (Asfaw et al., 1999; Heinzelin et al., 1999)
<i>Australopithecus africanus</i>	E	3.0–2.1 (McFadden et al., 1979; Partridge et al., 2000; Herries et al., 2013; Pickering and Herries, 2020)
<i>Australopithecus sediba</i>	E	2.0 (Pickering et al., 2011a, 2011b)
<i>Paranthropus aethiopicus</i>	C	2.7–2.3 (Harrison, 2002, 2011; Deino, 2011; McDougall et al., 2012; Wynn et al., 2020)
<i>Paranthropus robustus</i>	E	2.2–1.0 (Grine, 1989; Gibbon et al., 2014; Kuman et al., 2021)
<i>Paranthropus boisei</i>	C, D	2.5–1.3 (Walker et al., 1986; Kullmer et al., 1999; Dominguez-Rodrigo et al., 2013)
<i>Homo habilis</i>	B, C, E	2.3–1.4 (Kimbel et al., 1996; McDougall and Brown, 2006; Spoor et al., 2007a, 2007b)
<i>Homo rudolfensis</i>	C, D	2.3–1.9 (Feibel et al., 1989; McDougall and Brown, 2006; McDougall et al., 2012)
<i>Homo erectus</i> s.l. (Africa)	B, C, E	2.0–0.9 (Potts et al., 2004; Gathogo and Brown, 2006)
<i>Pan troglodytes</i>	C, F	1.7–Present (De Manuel et al., 2016)
<i>Pan paniscus</i>	F	1.7–Present (De Manuel et al., 2016)
<i>Gorilla gorilla</i>	F	0.5–Present (Scally et al., 2012)
<i>Gorilla beringei</i>	C, F	0.5–Present (Scally et al., 2012)

Abbreviations: A = Northcentral Africa, corresponding to Linder et al. (2012)'s Sudanian region; B = northern part of eastern Africa, corresponding to Linder et al. (2012)'s Somalian region; C = middle part of eastern Africa, corresponding to Linder et al. (2012)'s East African mosaic region; D = southern part of eastern Africa, corresponding to Linder et al. (2012)'s Zambezian region; E = South Africa, corresponding to Linder et al. (2012)'s southern African region; F = central Africa, corresponding to Linder et al. (2012)'s Congolian and Guinean regions; FAD = first-appearance datum; LAD = last-appearance datum.

<sup>a</sup> FADs and LADs, rounded to the nearest 0.1 Ma, are based on best estimates and do not include errors associated with the estimates. Most dates follow the review in Monge et al. (2022).

colonialism in Africa) and the differences in the geological settings of fossil-bearing sites in those regions. Ultimately, the results from our three-region analysis were mostly consistent with those of our six-region analysis (with one notable but qualified difference). Hence, we report the result of the three-partition analysis, together with further discussion in the [Supplementary Online Material \(SOM\) S1](#).

### 2.3. Dating the trees

A time-calibrated phylogeny is necessary to estimate the duration of each branch. This information is crucial for maximum likelihood analyses. We estimated the branch length for both trees using the minimum-branch-length method implemented in the R package 'paleotree' v. 3.3.25 (Bapst, 2012) with the argument 'mbl'. The minimum-branch-length estimate is often used in paleontological analysis since fossil specimens only provide a minimum age for each node (Hunt, 2013). In addition, this approach avoids the problem of artificial zero-length branches (Hunt and Carrano, 2010; Bapst, 2012; Soul and Friedman, 2015; Brocklehurst, 2016). Zero-length branches mean no inferred change between the tip and the node, thus creating a polytomy. This issue can be resolved by adding a minimum length to each zero-length branch (we used 0.1 Ma for this study). Node ages are estimated using the first appearance dates of the sister group of the clade. Based on the molecular data (Moorjani et al., 2016), we adjusted the minimum dates for the root of the trees (*Gorilla*–*Homo* node) and the *Pan*–*Homo* node to be 10.8 and 7.9 Ma, respectively. [Figures 2 and 3](#) show time-calibrated phylogenetic trees with alternative topologies.

### 2.4. Biogeographical analyses

We compared biogeographic models in the R package 'BioGeoBEARS' v. 1.1.2 (Matzke, 2013). 'BioGeoBEARS' implements likelihood versions of the biogeographic models, namely DIVA (Ronquist, 1997), DEC (Ree and Smith, 2008), and BayArea (Landis et al., 2013). The maximum likelihood versions of DIVA (DIVA-LIKE) and BayArea (BAYAREALIKE) have the same assumptions

about biogeographical processes described earlier but are implemented in a likelihood framework.

The base models used in this study are DIVALIKE, DEC, and BAYAREALIKE. These models have two free parameters that specify the rate of range expansion dispersal (parameter d) and range contraction extinction (parameter e) along the branches of the phylogenetic tree. In addition, three more models were created by adding a j parameter representing the 'founder-event' speciation at cladogenetic events (DIVALIKE+j, DEC+j, BAYAREALIKE+j). Although the founder-event speciation is a critical biogeographical process in several clades, particularly island clades (e.g., Mayr, 1954; Matzke, 2014), its significance in early hominin evolution is yet to be determined. Moreover, we modified each model by adding the x parameter to estimate the effect of distance on dispersal (i.e., whether the probability of dispersal increases as distance decreases), creating DIVALIKE+x, DIVALIKE+x+j, etc. We estimated the distance between geographic areas as the minimum distance measured in kilometers with FreeMapTools (<http://www.freemaptools.com/how-far-is-it-between.htm>).

In biogeographical analyses, the geographic range is treated as a character evolving along branches of the phylogenetic tree, similar to estimating ancestral character states for morphological or genetic data. However, unlike other ancestral character estimations, biogeographical analyses implemented in 'BioGeoBEARS' include a null range (i.e., a geographic range of 0 areas) in the anagenesis transition matrix. That is because range contraction (i.e., extinction) allows species to be present in no areas. Massana et al. (2015) found that models could underestimate extinction rates by allowing the null range to exist. We, therefore, compared models in which transitions into the null range in the transition rate matrix are prohibited (indicated by an asterisk in the abbreviated name of the models). These modified models are DIVALIKE\*, DIVALIKE\*+j, etc.

The models can sometimes mistakenly reconstruct widespread ancestors at the nodes. This could happen when extinction is inferred to be low in trees with long branches. A long branch represents a surviving lineage. If the extinction rate is high, lineage survival along the long branches will become unlikely. The consequence of a low extinction rate is inferring widespread ancestors. For example, if two daughter species each occupy a distinct region

(e.g., A and B), inferring a single-area ancestor (e.g., A) would mean that one of the descendants should have first expanded its range (B→AB) and then gone extinct (AB→B). Consequently, vicariance can explain the presence of widespread ancestors with disjunct descendants without invoking extinction events (Ree et al., 2005). Therefore, the allopatric realizations of DIVA and DEC tend to reconstruct widespread ancestors (ancestral regions which include all regions occupied by their descendants) at deeper nodes, particularly the root node. The widespread ancestors will subsequently break up by vicariance to produce daughter species with smaller ranges (Kodandaramaiah, 2010; Buerki et al., 2011).

The tendency to reconstruct wide ancestors in biogeographical analyses is called the 'ancestral area paradox' (Bremer, 1992, 1995; Ronquist, 1997; Ree et al., 2005). According to this paradox, ancestral regions are more widespread than their descendants in biogeographical analyses. The 'ancestral area paradox' contradicts the 'uniformitarianism principle' that the range distribution of the ancestors should resemble the descendants to a certain extent (Ree et al., 2005). Two approaches have been offered to avoid this problem (Ronquist, 1997; Kodandaramaiah, 2010). The first is to include sister taxa as outgroups. The other solution is to constrain the maximum number of areas occupied by ancestors. We set the maximum number of ancestral areas to three to reflect the maximum distribution of the extinct hominins at the tips of the trees. Overall, we tested 24 models for each tree that varied in the number and types of free parameters (Tables 3 and 4). We estimated the relative fit of each model using the sample-size-corrected Akaike information criterion and the relative weight of each model (Burnham and Anderson, 2002).

We estimated the number and types of biogeographic events using biogeographical stochastic mapping (BSM; Dupin et al., 2017). Stochastic mapping is a simulation method that provides possible histories of trait changes (e.g., morphological traits or mutations)

along the branches of the phylogenetic tree (Nielsen, 2002; Hulsenbeck et al., 2003; Ree, 2005; Bollback, 2006). Biogeographical stochastic mapping simulates biogeographical events conditioned on the phylogenetic tree, the observed range data, the biogeographical model, and the estimated parameters. We can estimate biogeographical event frequencies by generating stochastic maps and taking the mean and confidence interval. We ran 100 biogeographical stochastic maps in 'BioGeoBEARS' for the best-fitted model of each tree. Tables, phylogenetic trees, and R code are available on GitHub at [https://github.com/yeganehsekhavati/hominin\\_biogeography](https://github.com/yeganehsekhavati/hominin_biogeography).

### 3. Results

#### 3.1. Comparison of different models

Variation in the cladogenetic and anagenetic assumptions had little impact on the model performance (only somewhat changing the log-likelihood). However, modifying the baseline models by prohibiting the null range resulted in more refined models that better fit the data. The observed parameter estimates and the relative fit of each model for both trees (Figs. 2 and 3) are presented in Tables 3 and 4. For tree 1 (in which *A. sediba* is the sister taxon of *A. africanus*), the BAYAREALIKE\* model was the best approximating model, followed closely by BAYAREALIKE\*+j. Conversely, for tree 2 (in which *A. sediba* is the sister taxon of *Homo*), the model with the lowest size-corrected Akaike information criterion score was BAYAREALIKE\*+j, and the second-best approximating model was BAYAREALIKE\*. Notably, the likelihood of BAYAREALIKE+j+x\* with an additional distance parameter was not substantially lower in either tree.

Under the best approximating model for tree 1 (BAYAREALIKE\*), the rates of dispersal and extinction were inferred to be 0.13 and 0.57, respectively. The dispersal rate for the best approximating

**Table 3**  
Results of model comparison for tree 1.<sup>a,b</sup>

Models	Parameters				Log-likelihood	AICc	AICc weights	
	Number	d <sup>(1)</sup>	e <sup>(2)</sup>	j <sup>(3)</sup>				
DEC*	2	0.37	1.49	0.00	0.00	-51.53	107.92	0.03
DEC+j*	3	0.37	1.49	0.00	0.00	-51.53	110.90	0.01
DIVALIKE*	2	0.61	2.30	0.00	0.00	-52.78	110.42	0.01
DIVALIKE+j*	3	0.61	2.30	0.00	0.00	-52.78	113.41	0.00
BAYAREALIKE*	2	<b>0.13</b>	<b>0.57</b>	<b>0.00</b>	<b>0.00</b>	<b>-49.25</b>	<b>103.36</b>	<b>0.32</b>
BAYAREALIKE+j*	3	<b>0.08</b>	<b>0.30</b>	<b>0.04</b>	<b>0.00</b>	<b>-47.83</b>	<b>103.51</b>	<b>0.30</b>
DEC	2	0.13	0.11	0.00	0.00	-54.25	113.35	0.00
DEC+j	3	0.10	0.07	0.05	0.00	-53.25	114.34	0.00
DIVALIKE	2	0.15	0.13	0.00	0.00	-55.99	116.85	0.00
DIVALIKE+j	3	0.13	0.10	0.02	0.00	-55.72	119.28	0.00
BAYAREALIKE	2	0.11	0.33	0.00	0.00	-55.11	115.08	0.00
BAYAREALIKE+j	3	0.05	0.11	0.05	0.00	-50.58	109.01	0.02
DEC+x*	3	4.87	0.50	0.00	-0.41	-49.33	106.50	0.07
DEC+j+x*	4	2.86	0.41	0.39	-0.37	-49.29	109.91	0.01
DIVALIKE+x*	3	3.64	0.62	0.00	-0.36	-49.87	107.58	0.04
DIVALIKE+j+x*	4	3.15	4.97	0.03	-0.12	-53.09	117.51	0.00
BAYAREALIKE+x*	3	4.50	0.40	0.00	-0.49	-49.17	106.18	0.08
BAYAREALIKE+j+x*	4	4.50	0.30	0.68	-0.50	-47.20	105.74	0.10
DEC+x	3	4.57	0.10	0.00	-0.46	-53.03	113.90	0.00
DEC+j+x	4	4.51	0.07	1.37	-0.48	-51.99	115.32	0.00
DIVALIKE+x	3	0.96	0.12	0.00	-0.24	-55.34	118.52	0.00
DIVALIKE+j+x	4	4.50	0.10	0.64	-0.45	-54.54	120.41	0.00
BAYAREALIKE+x	3	3.14	0.33	0.00	-0.43	-54.51	116.87	0.00
BAYAREALIKE+j+x	4	4.26	0.11	0.82	-0.55	-50.06	111.46	0.01

Abbreviations: AICc = size-corrected Akaike information criterion; DEC = dispersal-extinction-cladogenesis model; DIVALIKE = likelihood interpretation of dispersal-vicariance analysis; BAYAREALIKE = likelihood interpretation of Bayesian inference of historical biogeography for many discrete areas; d<sup>(1)</sup> = rate of range expansion dispersal per million years, e<sup>(2)</sup> = rate of range contraction extinction per million years, j<sup>(3)</sup> = relative probability of jump dispersal, and x<sup>(4)</sup> = dispersal probability (as a function of distance in kilometers).

<sup>a</sup> The best approximating and second-best approximating models are shown in bold.

<sup>b</sup> Models marked by an asterisk are those in which we set the null area as false.

**Table 4**Results of model comparison for tree 2.<sup>a,b</sup>

Models	Number	Parameters				Log-likelihood	AICc	AICc weights
		d <sup>(1)</sup>	e <sup>(2)</sup>	j <sup>(3)</sup>	x <sup>(4)</sup>			
DEC*	2	1.29	4.70	0.00	0.00	-53.45	111.76	0.02
DEC-j*	3	1.18	4.57	1.39	0.00	-53.44	114.72	0.01
DIVALIKE*	2	0.28	0.91	0.00	0.00	-51.77	108.40	0.12
DIVALIKE+j*	3	0.27	0.91	0.01	0.00	-51.75	111.35	0.03
BAYAREALIKE*	2	<b>0.25</b>	<b>1.16</b>	<b>0.00</b>	<b>0.00</b>	<b>-51.53</b>	<b>107.92</b>	<b>0.15</b>
BAYAREALIKE+j*	3	<b>0.09</b>	<b>0.31</b>	<b>0.04</b>	<b>0.00</b>	<b>-49.17</b>	<b>106.20</b>	<b>0.37</b>
DEC	2	0.14	0.13	0.00	0.00	-56.13	117.13	0.00
DEC+j	3	0.10	0.07	0.06	0.00	-53.89	115.63	0.00
DIVALIKE	2	0.16	0.13	0.00	0.00	-57.39	119.65	0.00
DIVALIKE+j	3	0.13	0.10	0.04	0.00	-56.24	120.32	0.00
BAYAREALIKE	2	0.11	0.34	0.00	0.00	-55.96	116.78	0.00
BAYAREALIKE+j	3	0.06	0.11	0.05	0.00	-52.07	111.98	0.02
DEC-x*	3	4.94	0.87	0.00	-0.37	-50.77	109.39	0.07
DEC+j+x*	4	4.41	0.38	0.98	-0.42	-50.03	111.39	0.03
DIVALIKE x*	3	1.77	0.77	0.00	-0.25	-51.20	110.25	0.05
DIVALIKE+j+x*	4	4.08	0.68	0.36	-0.37	-50.82	112.97	0.01
BAYAREALIKE+x*	3	1.01	0.85	0.00	-0.34	-53.17	114.19	0.01
BAYAREALIKE+j+x*	4	1.16	0.31	0.37	-0.32	-48.73	108.79	0.10
DEC+x	3	0.01	0.01	0.00	0.00	-74.99	157.82	0.00
DEC+j+x	4	4.37	0.08	1.42	-0.47	-52.72	116.77	0.00
DIVALIKE+x	3	0.96	0.12	0.00	-0.23	-56.83	121.52	0.00
DIVALIKE j+x	4	2.57	0.09	0.57	-0.38	-55.28	121.88	0.00
BAYAREALIKE+x	3	3.15	0.34	0.00	-0.42	-55.36	118.58	0.00
BAYAREALIKE+j+x	4	0.07	0.78	0.40	0.33	-70.71	152.76	0.00

Abbreviations: AICc = size-corrected Akaike information criterion; DEC = dispersal-extinction-cladogenesis model; DIVALIKE = likelihood interpretation of dispersal-vicariance analysis; BAYAREALIKE = likelihood interpretation of Bayesian inference of historical biogeography for discrete areas; d<sup>(1)</sup> = rate of range expansion dispersal per million years, e<sup>(2)</sup> = rate of range contraction extinction per million years, j<sup>(3)</sup> = relative probability of jump dispersal, and x<sup>(4)</sup> = dispersal probability (as a function of distance in kilometers).

<sup>a</sup> The best approximating and second best approximating models are shown in bold.

<sup>b</sup> Models marked by an asterisk are those in which we set the null area as false.

model of the second tree (BAYAREALIKE\*+ j) was 0.09, and the extinction rate was 0.31. [Massana et al. \(2015\)](#) suggested treating the rate parameters as nuisance parameters rather than parameters of interest. Still, high rates of extinction and dispersal could lower the accuracy of biogeographical inferences ([Lieberman, 2002](#); [Ree and Smith, 2008](#); [Matzke, 2014](#)).

Toward deeper nodes, the ancestral estimation of BAYAREALIKE\* (best approximating model for tree 1 and second best approximating model for tree 2) and BAYAREALIKE\*+ j (best approximating model for tree 2 and second best approximating model for tree 1) yielded similar results. The estimated ancestral nodes deviated slightly within the 'upper' half of the trees, based on the choice of the model. Nevertheless, the general pattern is that BAYAREALIKE\* preferred broad ancestral ranges, whereas BAYAREALIKE\*+ j favored narrow ancestral ranges. For almost all nodes, the BAYAREALIKE\* estimates in tree 1 were comparable with BAYAREALIKE\* in tree 2. The same applies to BAYAREALIKE\*+ j estimates in both trees (detailed information is provided in [Table 4](#)). Since we consistently observed the aforementioned pattern, we report the result of the best approximating model in which we have the greatest confidence for each tree. Information on the estimated ancestral area based on the second-best approximating model is also included in [Table 5](#).

### 3.2. Ancestral area analyses

[Table 5](#) shows the results of ancestral character estimations and their probabilities for both trees. We report the most likely and the second most likely scenarios only if either has a probability of more than 20%. For each node in each tree, the most likely ancestral areas occupied by any given LCA according to the best-supported biogeographic model are depicted in [Figures 5 and 6](#), but these figures are simplifications that mask some of the biogeographic nuance elucidated in [Table 5](#) and are described in the following.

**Ancestral range estimation for tree 1** Based on the best approximating model (BAYAREALIKE\*, [Fig. 5](#)), the ancestral estimation for the LCA of gorillas and humans at the root of the tree is ambiguous. The two most favored ancestral ranges for the ancestor of *G. gorilla* and *G. beringei* are central Africa (61%) or, with a lower probability, central and eastern Africa<sub>Middle</sub> (27%). Collectively, the probability that at least part of the ancestral population occupied central Africa is ≥88%. Northcentral Africa was the region most likely occupied by the ancestor of the *Homo–Pan* clade, with a probability of 48%. Central Africa was the preferred ancestral range for the ancestor of *Pa. troglodytes* and *Pa. paniscus*, with a 53% probability.

Northcentral Africa was the most likely ancestral region for the ancestor of *Sahelanthropus* and later hominins (68%). The results suggest that the ancestors for the subsequent three nodes (the common ancestors of *Ardipithecus* and later hominins, *Australopithecus* and later hominins, and *A. afarensis* and later hominins) were most likely distributed in eastern Africa<sub>North</sub> and Middle (52%, 60%, and 52%, respectively) or less likely in Northcentral and eastern Africa<sub>North</sub> and Middle (23%, 21%, and 24%, respectively). Collectively, the probability that at least part of the ancestral population inhabited eastern Africa<sub>North</sub> and Middle ranged from ≥75% to 81%. The ancestor of *A. garhi* and later hominins was suggested to have occupied eastern Africa<sub>North</sub> and Middle and southern Africa (43%) or eastern Africa<sub>North</sub> and Middle (23%), meaning that the probability that at least some part of the ancestral population occupied eastern Africa<sub>North</sub> and Middle is ≥66%.

Nearly all of the remaining ancestors in the tree are likely to have occupied at least southern Africa and eastern Africa<sub>Middle</sub>, with eastern Africa<sub>North</sub> being the next most likely region to be added to that range. The exceptions to this pattern are *P. aethiopicus* and *P. boisei* and their LCA. The probability that the LCA of *P. aethiopicus* and *P. boisei* inhabited at least eastern Africa<sub>Middle</sub> is ≥72%, with the probability that it was also found in southern Africa being only 37%.

Table 5

Estimated ancestral geographic areas and their probabilities for each tree under the best approximating and second-best approximating models.<sup>a</sup>

Nodes	Tree1 (BAYAREALIKE*)	Tree 1 (BAYAREALIKE+j*)	Tree 2 (BAYAREALIKE*)	Tree 2 (BAYAREALIKE+j*)
Root	Unidentified	Unidentified	Unidentified	Unidentified
LCA of <i>G. gorilla</i> + <i>G. beringei</i>	<b>F: 0.61</b> ; CF: 0.27 (at least F: <b>≥0.88</b> )	<b>F: 0.58</b> ; CF: 0.37 (at least F: <b>≥0.95</b> )	<b>F: 0.61</b>	<b>F: 0.55</b> ; CF: 0.34 (at least F: <b>≥0.89</b> )
LCA of <i>Pan</i> + hominins	A: 0.48	A: 0.23	A: 0.37	A: 0.23
LCA of <i>Pa. troglodytes</i> + <i>Pa. paniscus</i>	<b>F: 0.53</b>	<b>F: 0.51</b>	F: 0.37	F: 0.49
LCA of <i>Sahelanthropus</i> + later hominins	<b>A: 0.68</b>	A: 0.43	<b>A: 0.62</b>	A: 0.44
LCA of <i>Ardipithecus</i> + later hominins	<b>BC: 0.52</b> ; ABC: 0.23 (at least BC: <b>≥0.75</b> )	<b>BC: 0.75</b>	BC: 0.22; C: 0.20 (at least C: <b>≥0.42</b> )	<b>BC: 0.71</b>
LCA of <i>Australopithecus</i> + later hominins	<b>BC: 0.60</b> ; ABC: 0.21 (at least BC: <b>≥0.81</b> )	<b>BC: 0.78</b>	BC: 0.26; C: 0.19 (at least C: <b>≥0.45</b> )	<b>BC: 0.73</b> ; ABC: 0.22 (at least BC: <b>≥0.95</b> )
LCA of <i>A. afarensis</i> + later hominins	<b>BC: 0.52</b> ; ABC: 0.24 (at least BC: <b>≥0.76</b> )	<b>BC: 0.67</b> ; ABC: 0.27 (at least BC: <b>≥0.94</b> )	BC: 0.22; C: 0.19 (at least C: <b>≥0.41</b> )	<b>BC: 0.59</b> ; ABC: 0.32 (at least BC: <b>≥0.91</b> )
LCA of <i>A. garhi</i> + later hominins	BCE: 0.43; BC: 0.23 (at least BC: <b>≥0.66</b> )	BC: 0.42; B: 0.29 (at least B: <b>≥0.71</b> )	BCE: 0.21; BC: 0.16 (at least BC: <b>≥0.41</b> )	B: 0.40; BC: 0.22 (at least B: <b>≥0.62</b> )
LCA of <i>A. africanus</i> + later hominins	—	—	BCE: 0.23; CE: 0.19 (at least CE: <b>≥0.42</b> )	<b>E: 0.81</b>
LCA of <i>A. sediba</i> + <i>A. africanus</i> clade + later hominins	BCE: 0.41; CE: 0.28 (at least CE: <b>≥0.69</b> )	<b>E: 0.54</b> ; BC: 0.27	—	—
LCA of <i>A. sediba</i> + <i>A. africanus</i>	BCE: 0.29; CE: 0.26; E: 0.25 (at least CE: <b>≥0.55</b> )	<b>E: 0.96</b>	—	—
LCA of <i>Paranthropus</i> + later hominins	BCE: 0.39; CE: 0.39 (at least CE: <b>≥0.78</b> )	E: 0.39; BC: 0.25	CE: 0.25; BCE: 0.22; C: 0.21 (at least CE: <b>≥0.47</b> ; <b>At least C: ≥0.68</b> )	<b>E: 0.77</b>
LCA of <i>Paranthropus</i> clade	CE: 0.48; BCE: 0.26 (at least CE: <b>≥0.76</b> )	E: 0.42; C: 0.26	C: 0.28; CE: 0.27 (at least C: <b>≥0.55</b> )	<b>E: 0.72</b>
LCA of <i>P. aethiopicus</i> and <i>P. boisei</i>	CE: 0.37; C: 0.35 (at least C: <b>≥0.72</b> )	<b>C: 0.76</b>	C: 0.44; CE: 0.22 (at least C: <b>≥0.66</b> )	<b>C: 0.84</b>
LCA of <i>A. sediba</i> + <i>Homo</i>	—	—	CE: 0.33; BCE: 0.20 (at least CE: <b>≥0.52</b> )	<b>E: 0.62</b>
LCA of <i>Homo</i> clade	BCE: 0.44; CE: 0.29 (at least CE: <b>≥0.73</b> )	BCE: 0.27; CE: 0.24; BC: 0.21 (at least CE: <b>≥0.51</b> ; at least BC: <b>≥0.48</b> )	CE: 0.31; BCE: 0.20 (at least CE: <b>≥0.51</b> )	CE: 0.33; E: 0.21 (at least E: <b>≥0.51</b> )
LCA of <i>H. ergaster</i> and <i>H. habilis</i>	<b>BCE: 0.56</b> ; CE: 0.23 (at least CE: <b>≥0.79</b> )	<b>BCE: 0.50</b>	CE: 0.26; BCE: 0.25 (at least CE: <b>≥0.51</b> )	BCE: 0.34; CE: 0.27 (at least CE: <b>≥0.61</b> )

Abbreviations: BAYAREALIKE = likelihood interpretation of Bayesian inference of historical biogeography for discrete areas; LCA = last common ancestor; A = Northcentral Africa; B = northern part of eastern Africa; C = middle part of eastern Africa; D = southern part of eastern Africa; E = southern Africa; F = central Africa.

<sup>a</sup> Probabilities are shown if they are more than 20%. Probabilities greater than 50% (meaning that a given estimation is more likely than not) are highlighted in bold.

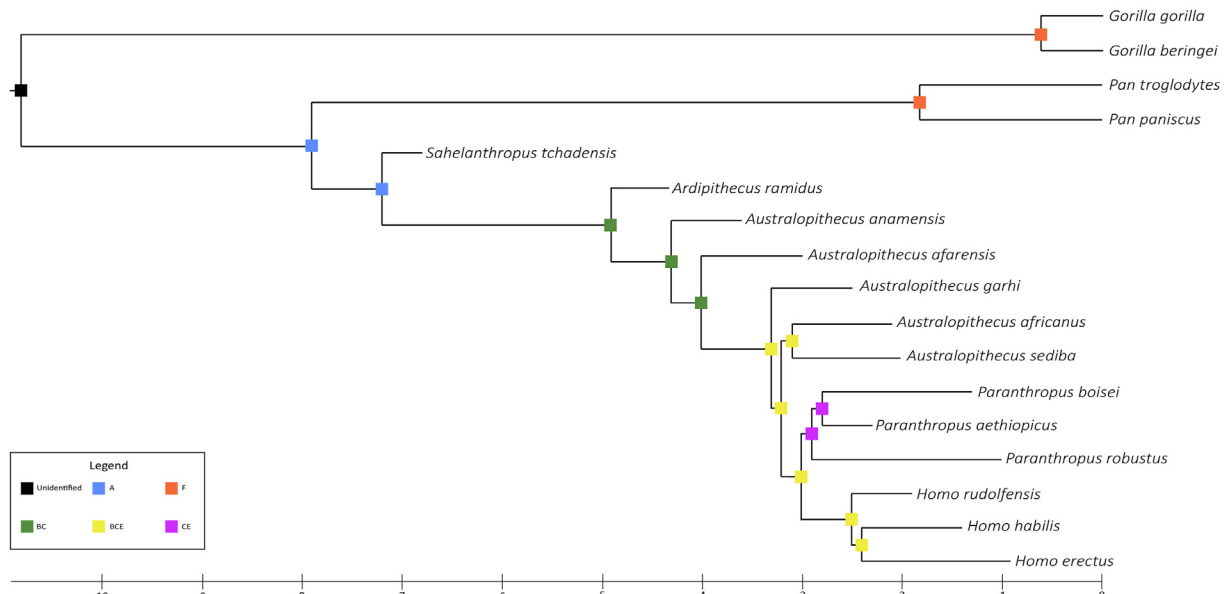


**Figure 5.** Most probable ancestral range estimation in Tree 1 using the best approximating model, namely, the maximum-likelihood version of BayArea that does not allow transitions into the null range (BAYAREALIKE\*). Colors represent the areas occupied by each LCA, and may correspond to single regions or multiple regions. Regions: A = Northcentral Africa; B = northern part of eastern Africa; C = middle part of eastern Africa; D = southern part of eastern Africa; E = southern Africa; F = central Africa (For interpretation of the references to color in this figure legend, the reader is referred to the web version of this article). Abbreviation: LCA = last common ancestor.

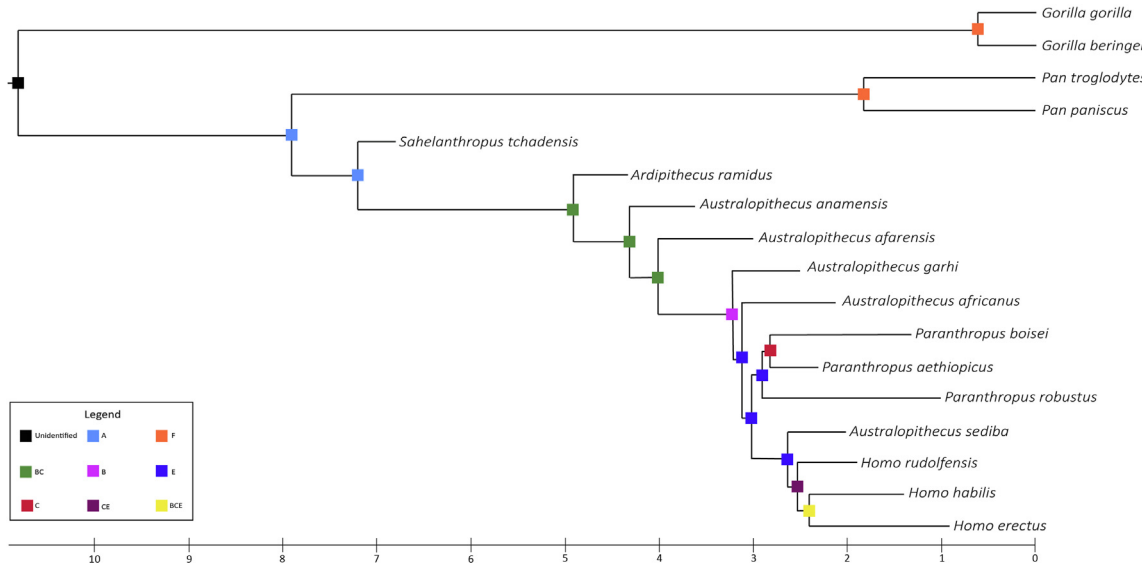


**Figure 6.** Most probable ancestral range estimation in Tree 2, using the best approximating model, namely, the maximum likelihood version of BayArea that does not allow transitions into the null range (BAYAREALIKE\*+j). Colors represent the areas occupied by each last common ancestor, and may correspond to single regions or multiple regions. Regions: A = Northcentral Africa; B = northern part of eastern Africa; C = middle part of eastern Africa; D = southern part of eastern Africa; E = southern Africa; F = central Africa (For interpretation of the references to color in this figure legend, the reader is referred to the web version of this article).

**Ancestral range estimation for tree 2** As in tree 1, the best approximating model of tree 2 (BAYAREALIKE\*+j) found (Table 5; Fig. 6) that the ancestral region at the root of the phylogenetic tree was ambiguous. The subsequent 7 nodes yielded the same most likely scenarios as tree 1 (Table 5). Eastern Africa<sub>North</sub> and eastern Africa<sub>North</sub> and Middle were inferred as the ancestral regions of *A. garhi* and later hominins (40% and 22%, respectively). The probability that at least part of the ancestral population inhabited eastern Africa<sub>North</sub> is  $\geq 62\%$ . All of the remaining ancestors in the tree, except for the last two nodes, are likely to have occupied either southern Africa or eastern Africa<sub>Middle</sub>. For the ancestor of *Homo*, the results suggested that eastern Africa<sub>Middle</sub> and southern Africa (33%) followed by southern Africa (21%) were the most probable regions. The probability that at least part of the ancestral population occupied southern Africa is  $\geq 51\%$ . Finally, similar to tree 1, there are two probable candidates for the ancestral region of *H. ergaster* and *H. habilis*: eastern Africa<sub>North</sub> and Middle and southern Africa (34%) and eastern Africa<sub>Middle</sub> and southern Africa (27%). The probability that at least part of the population occupied eastern Africa<sub>Middle</sub> and southern Africa is  $\geq 61\%$ .

### 3.3. Biogeographic stochastic mapping and biogeographic processes

Table 6 shows the means and 95% confidence intervals of cladogenetic event counts from 100 BSMs. All cladogenetic events in tree 1 and 72% of events in tree 2 are sympatry (Table 6). For tree 1, within-area speciation happened more frequently in eastern Africa<sub>North</sub> and Middle and southern Africa (18%), eastern Africa<sub>Middle</sub> and southern Africa (16%), and eastern Africa<sub>North</sub> and Middle (16%).

For tree 2, most within-area speciation appeared to have occurred in eastern Africa<sub>North</sub> and Middle (18%) and southern Africa (18%).

BAYAREALIKE models do not incorporate vicariance events (Fig. 1); therefore, under these models, no vicariance events were inferred for either tree 1 or 2. Jump dispersal or founder events comprised 28% of cladogenesis events in tree 2 (Table 6) and were most commonly retrieved from the following nodes: LCA of *A. garhi* and later hominins (19%), LCA of *Paranthropus* (18%), and LCA of *Homo* (11%). Although jump dispersals were also inferred at the root of the favored model in tree 2 (Table 7), it did not have strong support based on the results of BSM (it only occurred 5% of the time).

The results from both trees suggested that range expansion dispersals happened frequently. Movement patterns did not seem to differ substantially across regions (Tables 8 and 9). The highest range expansion dispersals in both trees involved movements from eastern Africa<sub>Middle</sub> to eastern Africa<sub>South</sub> (8% and 9%, respectively) and central Africa to eastern Africa<sub>Middle</sub> (7% and 10%, respectively). Overall, eastern Africa<sub>Middle</sub> was the source of most estimated dispersals (29% for tree 1 and 30% for tree 2), followed by central Africa (17% and 19%, respectively). Dispersals were almost evenly distributed across destinations. Eastern Africa<sub>Middle</sub> was also the destination of most estimated dispersals (20% and 28%, respectively), closely followed by eastern Africa<sub>North</sub> (19% for both trees).

## 4. Discussion

Historical biogeography has moved away from observing patterns of species distribution to incorporating biogeographic

**Table 6**

Means of cladogenetic event counts from 100 biogeographical stochastic mappings with 95% confidence intervals in parentheses. Cladogenesis events inferred at internal nodes of the phylogenetic tree. Sixteen cladogenetic events are inferred for 16 internal nodes in each tree. Sympatry makes up 100% of inferred cladogenetic events in tree 1 and 72% in tree 2. Twenty-eight percent of other cladogenesis events in tree 2 are inferred to be founder events. Confidence intervals are shown in parentheses.

Phylogenetic tree	Widespread and narrow sympatry	Subset sympatry	Jump dispersal	Vicariance	Total cladogenetic events
Tree 1	16 (0)	0	0	0	16
Tree 2	11.53 (11.29–11.77)	0	4.47 (4.23–4.71)	0	16

**Table 7**

Estimated ancestral range<sup>a</sup> and biogeographical processes in the branch leading up to a given node (representing a last common ancestor) and in the branches derived from that node, under the best approximating model for each tree.<sup>c</sup>

Nodes	Tree 1 (BAYAREALIKE*)	Tree 2 (BAYAREALIKE+j*)
Root <sup>b</sup>		
LCA of <i>G. gorilla</i> + <i>G. beringei</i>	A* → A, A** → F, A*** (sympathy)	A → F, A → F, A (jump dispersal)
LCA of <i>Pan</i> + hominins	F → F, F → F, CF (sympathy)	F → F, F → F, CF (sympathy)
LCA of <i>Pa. troglodytes</i> + <i>Pa. paniscus</i>	A → A, A → F, A (sympathy)	A → A, A → F, A (sympathy)
LCA of <i>Sahelanthropus</i> + later hominins	F → F, F → CF, F (sympathy)	F → F, F → CF, F (sympathy)
LCA of <i>Ardipithecus</i> + later hominins	A → A, A → A, BC (sympathy)	A → A, A → A, BC (sympathy)
LCA of <i>A. anamensis</i> + later hominins	BC → BC, BC → BC, BC (sympathy)	BC → BC, BC → BC, BC (sympathy)
LCA of <i>A. afarensis</i> + later hominins	BC → BC, BC → BC, BC (sympathy)	BC → BC, BC → ABC, B (sympathy)
LCA of <i>A. garhi</i> + later hominins	BC → BC, BC → ABC, BCE (sympathy)	B → B, E → B, E (jump dispersal)
LCA of <i>A. africanus</i> + later hominins	BCE → BCE, BCE → B, BCE (sympathy)	E → E, E → E, E (sympathy)
LCA of <i>A. sediba</i> + <i>A. africanus</i> clade + later hominins	—	—
LCA of <i>A. sediba</i> + <i>A. africanus</i>	BCE → BCE, BCE → BCE, BCE (sympathy)	—
LCA of <i>Paranthropus</i> + later hominins	BCE → BCE, BCE → E, E (sympathy)	—
LCA of <i>Paranthropus</i>	BCE → BCE, BCE → CE, BCE (sympathy)	E → E, E → E, E (sympathy)
LCA of <i>P. aethiopicus</i> and <i>P. boisei</i>	CE → CE, CE → CE, E (sympathy)	E → C, E → C, E (jump dispersal)
LCA of <i>A. sediba</i> + <i>Homo</i>	CE → CE, CE → CD, C (sympathy)	C → C, C → CD, C (sympathy)
LCA of <i>Homo</i>	—	E → E, E → E, CE (sympathy)
LCA of <i>H. ergaster</i> and <i>H. habilis</i>	BCE → BCE, BCE → CD, BCE (sympathy)	CE → D, CE → CD, BCE (jump dispersal)
	BCE → BCE, BCE → BCE, BCE (sympathy)	BCE → BCE, BCE → BCE, BCE (sympathy)

Abbreviations: A = Northcentral Africa; B = northern part of eastern Africa; C = middle part of eastern Africa; LCA = last common ancestor; D = southern part of eastern Africa; E = southern Africa; F = central Africa; BAYAREALIKE = likelihood interpretation of Bayesian inference of historical biogeography for discrete areas; j = relative probability of jump dispersal.

<sup>a</sup> For each node, we indicated the estimated ancestral region for the LCA of the node (single asterisk), followed by the estimated ancestral region for each lineage after the initial split (double asterisk), followed by the observed region occupied by the taxa at the tips of the trees (triple asterisk).

<sup>b</sup> Uncertainty is very high at the root, and any estimation is unreliable.

<sup>c</sup> The ancestral regions occupied by each LCA, as indicated by the best supported biogeographic model, are depicted in Figs. 5 and 6.

**Table 8**

Number of estimated anagenetic dispersal events among regions averaged across 100 biogeographical stochastic mappings in tree 1. Confidence intervals are shown in parentheses.

Region	A	B	C	D	E	F
A	0	0.90 (0.75–1.05)	1.04 (0.86–1.22)	0.67 (0.5–0.84)	0.54 (0.39–0.69)	0.96 (0.74–1.18)
B	0.92 (0.75–1.09)	0	1.07 (0.85–1.29)	0.58 (0.43–0.73)	1.16 (0.96–1.36)	0.76 (0.59–0.93)
C	1.29 (1.07–1.51)	1.88 (1.56–2.20)	0	2.18 (1.97–2.39)	1.56 (1.31–1.81)	1.27 (1.04–1.50)
D	0.25 (0.16–0.34)	0.50 (0.35–0.65)	0.64 (0.47–0.81)	0	0.46 (0.32–0.60)	0.58 (0.43–0.73)
E	0.52 (0.35–0.69)	1.06 (0.85–1.27)	0.70 (0.51–0.89)	0.73 (0.54–0.92)	0	0.72 (0.52–0.92)
F	0.73 (0.57–0.89)	0.83 (0.65–1.01)	2.01 (1.81–2.21)	0.55 (0.41–0.69)	0.67 (0.49–0.85)	0

Abbreviations: A = Northcentral Africa; B = northern part of eastern Africa; C = middle part of eastern Africa; D = southern part of eastern Africa; E = southern Africa; F = central Africa.

**Table 9**

Number of estimated anagenetic dispersal events among regions averaged across 100 biogeographical stochastic mappings in tree 2. Confidence intervals are shown in parentheses.

Region	A	B	C	D	E	F
A	0	0.48 (0.36–0.6)	0.40 (0.28–0.52)	0.19 (0.09–0.29)	0.22 (0.13–0.31)	0.43 (0.28–0.58)
B	0.71 (0.56–0.86)	0	1.16 (0.95–1.37)	0.29 (0.19–0.39)	0.53 (0.4–0.66)	0.39 (0.27–0.51)
C	0.90 (0.73–1.07)	1.3 (1.1–1.5)	0	1.72 (1.57–1.87)	0.77 (0.57–0.97)	0.92 (0.72–1.12)
D	0.15 (0.07–0.23)	0.24 (0.15–0.33)	0.71 (0.56–0.86)	0	0.25 (0.16–0.34)	0.40 (0.28–0.52)
E	0.20 (0.12–0.28)	1.09 (1.03–1.15)	1.1 (0.93–1.27)	0.37 (0.27–0.47)	0	0.35 (0.24–0.46)
F	0.47 (0.33–0.61)	0.54 (0.41–0.67)	1.89 (1.72–2.06)	0.40 (0.27–0.53)	0.33 (0.22–0.44)	0

Abbreviations: A = Northcentral Africa; B = northern part of eastern Africa; C = middle part of eastern Africa; D = southern part of eastern Africa; E = southern Africa; F = central Africa.

processes in probabilistic approaches. The limitations of conventional pattern-matching approaches for inferring biogeography have been widely studied (e.g., McDowell, 2004; Popper, 2005; Crisp et al., 2011a, 2011b; Faith et al., 2021). One limitation is that numerous alternative explanations can be consistent with an observation without rigorously comparing them (Faith et al., 2021). Moreover, previous efforts to infer hominin historical biogeography in a phylogenetic framework (Strait and Wood, 1999; Strait, 2013) used a parsimony-based method that ignores critical information about time.

Regardless of the method used, various biases in paleontological data can affect the results of our study. One such bias is the limited

number of available fossils. Species represented by a few specimens from one region (e.g., *A. garhi*) pose a challenge to understanding the overall distribution of taxa simply because there is too little information to determine their presence in broader geographical contexts. This limitation may affect the accuracy and reliability of the present study (Su and Harrison, 2008). Additionally, taphonomic biases (Behrensmeyer and Reed, 2013) and sporadic sampling (Maxwell et al., 2018) can significantly affect the preservation and restoration of fossils, which could result in an incomplete representation of the fossil taxa. Therefore, when interpreting our results, it is important to consider the uneven distribution of fossils across different geographic regions. A high concentration of fossils

in certain areas could create a misconception that those areas played a more significant role in the evolution of hominins than they actually did. On the other hand, areas with lower fossil density may not be given enough consideration. This uneven distribution of fossils is due to variations in geology and also reflects historical biases in paleontological research, including the impact of colonialism (Faith et al., 2021; Raja et al., 2022; Wood and Smith, 2022). Colonialism is intricately linked with geographic data used to study taxa distribution in biogeographical studies (Monarrez et al., 2022). Consequently, taxa are geographically dispersed in a biased manner, particularly in Africa, where poorer regions are often considered data-deficient (Eichhorn et al., 2020).

Furthermore, the taxonomic assignment of hominin fossils is often highly debated (Wood and Boyle, 2016), and taxonomic attributions can significantly impact modeling results. There is also phylogenetic uncertainty that can impact our result. Although we considered the uncertainty in the phylogenetic position of *A. sediba* in our study, it is important to recognize that the phylogenetic positions of numerous hominin taxa remain controversial (Strait and Grine, 2004; Monge et al., 2019; Martin et al., 2021). Despite these limitations, paleontological datasets remain the only tangible record of life's history of diversity, and including fossils improves biogeographical inferences (Lieberman, 2002).

Earlier, we acknowledged that there is no definitive or 'correct' way to define regions in biogeographic analyses. Using modern data to identify biogeographic regions could introduce biases because such regions may have changed in the past due to environmental and climate changes. For example, Raia et al. (2020) found that past extinctions of *Homo* species were linked to increased vulnerability to climatic change. Timmermann et al. (2022) also showed that changes in temperature and precipitation patterns had a significant role in shaping the distribution and persistence of archaic human populations and that the succession of these populations was influenced by changes in resource availability and competition. In addition, climate fluctuations can create ecological barriers by expanding and contracting habitats, leading to genetic differentiation between populations (Scerri et al., 2018). These studies highlight the importance of considering the role of climate change and past environments in understanding the evolution and distribution of species. In our study, we acknowledge the limitations of not including paleoenvironmental data, but such data are not known with equivalent levels of scale across all fossil hominin sites. Future studies can benefit from integrating environmental data to enhance biogeographic analyses and gain insight into the evolution and distribution of organisms (e.g., Folk et al., 2018; Naranjo et al., 2023) if standardization of ecological data can be achieved.

Each model examined in this study makes different assumptions about biogeographic processes and is optimal under different circumstances. These models can be helpful while considering the various assumptions underlying each model and how those assumptions might shape results. For example, BayArea assumes that ancestral ranges are inherited identically (sympatry) and do not accommodate vicariance. In contrast, the range inheritance scenario in DIVA and DEC allows daughter species to occupy subsets of the ancestral range, reflecting the notion that speciation is associated with subdivision (Fig. 1).

In all our analyses, we noticed that modifying the baseline models by prohibiting null ranges results in refined models that better fit the data. We also incorporated the  $x$  parameter to represent an increase in dispersal probability as distance decreases in half of the examined models. We found that the inclusion of this parameter slightly lowered the fit of the models. However, given

the small size of the tree, we may need more power to incorporate complex models with a greater number of parameters. Nevertheless, there is evidence to support the idea that the probability of dispersals increases as distance decreases (also see Foley, 2018). In most cases, the base rate of range expansion was higher in the  $+x$  models, indicating that the rate of dispersal was higher between nearby areas and lower between distant regions (also see Foley, 2018). In non- $x$  models, estimated dispersals were often much lower since these models have to fit a constant dispersal rate between all areas regardless of distance (Soto-Trejo et al., 2017).

Comparing 24 models for each tree suggested that BAYAREALIKE\* was the favored model for tree 1, in which *A. sediba* is the sister taxon of *A. africanus*. BAYAREALIKE\* $+j$  was the best approximating model for tree 2, in which we placed *A. sediba* as the sister taxon of *Homo* (Fig. 3). Uncertainty is associated with ancestral estimation for most nodes in both trees. It is most apparent at the root of both trees, where the ancestral region for the ancestor of gorillas and humans is unidentifiable. This ambiguity is partly due to the higher number of coding regions as the probabilities are more spread out over 41 possible ancestral ranges:  $\binom{6}{3} + \binom{6}{2} + \binom{6}{1} = 41$ . However, in some cases, the probability that at least one of our 6 regions was occupied is usually estimated to be high. For example, the most likely ancestral regions for the ancestor of *G. gorilla* and *G. beringei* are inferred to be central Africa (61% for tree 1; 55% for tree 2) and central to eastern Africa<sub>Middle</sub> (27% for tree 1; 34% for tree 2). Although both these probabilities are modest, the probability that at least part of the population inhabited central Africa is  $\geq 88\%$ .

Figures 5 and 6 show the maximum-likelihood ancestral range estimation for each tree using the best approximating models. Central Africa is the inferred region for the LCA of *Gorilla* and the LCA of *Pan*. This supports the idea that while the ancestors of gorillas and chimpanzees remained in western and central Africa, hominins eventually dispersed to eastern Africa (Strait, 2013). The results also suggest that Northcentral Africa was the most likely ancestral region for the LCA of the *Homo–Pan* clade and the LCA of *Sahelanthropus* and later hominins, making it a possible center of hominin origins. This finding corroborates the previous hypothesis by Strait (2013), who identified central Africa (west of the Rift Valley) as the ancestral region of the LCA of *S. tchadensis* and later hominins.

According to both trees, eastern Africa<sub>North and Middle</sub> was estimated to be the most probable ancestral region for the ancestors of, respectively, *Ardipithecus* and later hominins, *Australopithecus* and later hominins, and *A. afarensis* and later hominins. The study's results align with prior research by Strait (2013), who also suggested that hominins reached eastern Africa at this stage in their evolutionary history. Additionally, the Bahr el Ghazal specimen (Brunet et al., 1995) supports the notion of a westward dispersal from eastern Africa to Northcentral Africa, which is in agreement with prior investigations (Strait, 2013; Macho, 2015).

The biogeographic patterns revealed in trees 1 and 2 (Figs. 2 and 3) are influenced by the phylogenetic relationships of *A. sediba* as it affects whether hominin ancestors after about 3.3 Ma were widespread or endemic (taxa that occupy only one region; see Fattorini, 2017 for a discussion of the term endemism). A high level of narrow endemism seems to be common in Africa, particularly in Afrotropical areas, the coastal region of East Africa, and the South African Cape Region (Linder et al., 2012; also see Kier et al., 2009). Identifying endemism depends critically on the scale of analyses (Fattorini, 2017). In this paper, we identified endemic species as those restricted to one of our six regions. For example, both trees agreed that the LCA of

*Pan* + hominins and LCA of *Sahelanthropus* + later hominins were endemic to Northcentral Africa. At about 5 Ma, we no longer see endemic ancestors in Northcentral Africa. Widespread ancestors in eastern Africa<sub>North and Middle</sub> were inferred to be the ancestral region for several taxa at ~5–4 Ma.

Widespread ancestors in eastern<sub>North and Middle</sub> and southern Africa were inferred for all nodes after the branching of *A. afarensis* in tree 1 (except for the ancestor of the *Paranthropus* clade and the ancestor of *P. boisei* and *P. aethiopicus*). Although the probability that these ancestral species were present in eastern Africa<sub>North</sub> is low for these nodes, they likely occupied eastern<sub>Middle</sub> and southern Africa. Eastern<sub>Middle</sub> and southern Africa are also the regions inferred to be the most likely locations for the ancestor of *Paranthropus* clade and the ancestor of *P. boisei* and *P. aethiopicus*. This is in contrast to Strait's (2013) results that eastern Africa was the ancestral region for all these hominins, with three southward dispersals occurring along the branches leading to *A. africanus*, *P. robustus*, and *H. habilis*.

Moreover, tree 2 inferred endemic ancestors from 3.3 Ma until the origin of *Homo*. Consistent with Strait (2013), the ancestor of *A. garhi* and later hominins was inferred to be restricted to eastern Africa<sub>North</sub>. However, unlike Strait (2013), we inferred that nearly all of the remaining ancestors were most likely endemic to South Africa. We inferred a major southern dispersal before the emergence of the LCA of *A. africanus* and later hominins. After that, South Africa was part of all the inferred ancestral regions, except for the ancestor of *P. aethiopicus* and *P. boisei*, which lived in eastern Africa<sub>Middle</sub>. Strait (2013), however, suggested that during this time, two southward dispersals happened along the branches leading to *A. africanus* and *P. robustus*.

For the LCA of the *Homo* clade, tree 2 inferred widespread ancestors in eastern Africa<sub>Middle</sub> and southern Africa, although with low probability. However, it is more probable that at least some portion of the population occupied South Africa. The inferred distribution of the ancestor of *H. ergaster* and *H. habilis* was across eastern Africa<sub>North and Middle</sub> and southern Africa, with a low probability of presence in eastern Africa<sub>North</sub>, as suggested by tree 1. In contrast, while Strait (2013) suggested that eastern Africa was the ancestral region for both nodes and that *H. habilis* dispersed southward from East Africa, our inference based on tree 2 suggests that South Africa was the ancestral region or part of the ancestral region for nodes subsequent to the LCA of *A. sediba* and *Homo*. Furthermore, the dispersals that occurred after the origin of *Homo* were from southern Africa to eastern Africa, in the opposite direction of what Strait (2013) suggested.

Joordens et al. (2019) suggested that before ~3 Ma, there were widespread hominins across different parts of Africa, whereas after ~3 Ma, hominins were endemic. This is consistent with tree 2, in which we saw widespread ancestors before ~3 Ma (but also with the origin of *Homo*). They (Joordens et al., 2019) further argued that before ~3 Ma, the difference in hominin abundance between Laetoli, Afar, and Turkana Basins reflected an actual difference in hominin distribution. However, after ~3 Ma, a difference in hominin abundance in these sites may not reflect an actual difference in hominin distribution (also see Su and Harrison, 2008; Villaseñor et al., 2020).

#### 4.1. Patterns of sympatry, dispersal, and vicariance

We used stochastic mapping to examine the uncertainty associated with the biogeographical history of early hominins. Our analysis revealed that the most common cladogenetic events in both trees were widespread and narrow sympatry. In tree 1, all of the cladogenetic events were of this type, whereas in tree 2, this was the case for 72% of the events. This finding is consistent with

previous studies (Spoor et al., 2007a, 2007b; Schroer and Wood, 2015; Haile-Selassie et al., 2016; Macho, 2017), suggesting that sympatry played a crucial role in shaping hominin evolution. Moreover, studies on genetic data have suggested that hominins and the *Pan* lineage exchanged genes after their initial split (Patterson et al., 2006), implying sympatry. Similarly, there has been gene flow between the two gorilla species (Thalmann et al., 2007; Mailund et al., 2012; Scally et al., 2012) and probably between chimpanzees and bonobos (De Manuel et al., 2016; Kuhlwilm et al., 2019; but see Won and Hey, 2005; Caswell et al., 2008). Based on these data, nonallopatric speciation seems common in great apes (Mailund et al., 2012). Mailund et al. (2012) argued that gene flow within the two gorilla species and the *Homo*–*Pan* clade extended several hundred thousand years. On the contrary, *Pa. troglodytes* and *Pa. paniscus* experienced a clear split and showed a weak signal of gene flow. Therefore, they suggested allopatric mode speciation for bonobos and chimpanzees and nonallopatric speciation for *G. gorilla*–*G. beringei* and *Homo*–*Pan* (but see Webster, 2009). The biogeographic pattern inferred from our study is consistent with the hypothesis proposed by Mailund et al. (2012) that nonallopatric speciation could have occurred between humans and their close relatives.

It is unclear whether jump dispersals significantly influenced early hominin evolution. Based on the results of the stochastic mapping, only 28% of cladogenesis events in tree 2 were inferred to be caused by jump dispersals. The jump dispersals were inferred to occur at the LCAs of *A. garhi* and later hominins (19%), *Paranthropus* (18%), and *Homo* (11%), representing rapid dispersal to a new area outside the ancestral range. Jump dispersal seems more frequent in datasets with many endemic species (Dupin et al., 2017) and island clades (Matzke, 2014), whereas intracontinental groups with widespread taxa sometimes support models without jump dispersal (Berger et al., 2016).

Vrba (1992) suggested that one way to categorize biogeographical processes is to classify them as either active, such as dispersal, or passive, such as vicariance. From this perspective, a high number of anagenetic dispersals inferred from our study suggests that hominins often actively respond to ecological and environmental factors by expanding and contracting their ranges. Moreover, the movement patterns observed in both trees did not differ significantly across regions (Tables 8 and 9). Eastern Africa<sub>Middle</sub> was identified as the primary source of most estimated dispersals, followed by central Africa. Eastern Africa<sub>Middle</sub> was also the destination of most estimated dispersals, closely followed by eastern Africa<sub>North</sub>. These findings suggest that hominins were highly mobile and that their dispersals were not limited to any particular region or destination. The ability to move across regions and adapt to diverse environments may have played a significant role in hominin evolutionary history. Vicariance, on the other hand, was likely not a significant biogeographical process in early human evolution (contra Vrba, 1992; Trauth et al., 2010).

#### 4.2. The most likely scenario for early hominin biogeographic history

The biogeographic history of hominins is complex, and there is uncertainty surrounding many nodes. However, we can nonetheless broadly infer the most likely scenario involving early hominin distribution in Africa. We found that the LCA of the *Homo*–*Pan* clade originated in Northcentral Africa and that the LCA of *S. tchadensis* and other hominins remained in that region. The LCA of *Ar. ramidus* and later hominins dispersed to eastern Africa<sub>North and Middle</sub>, which was also the range occupied by the LCA of *Australopithecus* and later hominins, as well as the LCA of *A. afarensis* and later hominins. These findings were consistent across both trees.

Biogeographic reconstructions at higher internal nodes differed according to whether *A. sediba* was the sister taxon of *A. africanus* or *Homo*. A key difference between these two reconstructions concerned the degree to which LCAs were endemic to only one region or occupied multiple regions (Table 5; Figs. 5 and 6). However, a common feature of both reconstructions is that most, if not all, of these LCAs occupied South Africa, and this region is therefore identified as a key locus of species origination. Overall, our results provide new insights into the complex biogeographic history of hominins and emphasize the importance of further research to better understand the evolutionary processes that have shaped hominin distribution over time.

Lastly, by examining our best approximating models for each tree and comparing them to those of *Strait (2013)*, we identified certain outcomes that were in agreement. Similar to *Strait (2013)*, we identified an early eastern dispersal from (north)central Africa at the branch leading to *Ar. ramidus*. Furthermore, our study also inferred a hominin dispersal toward southern Africa prior to ~3 Ma, which is consistent with *Strait (2013)*'s suggestion of a southern dispersal by *A. africanus* or its immediate ancestor. However, we inferred that this southward dispersal most likely happened before or at the LCA of *A. garhi* and later hominins.

However, our study's findings did not support some of *Strait (2013)*'s predictions. For instance, *Strait (2013)* suggested a southward dispersal for *P. robustus* or its ancestor, but our results based on both trees showed that the ancestor of the *Paranthropus* clade had already occupied South Africa, where *P. robustus* remained. Additionally, *Strait (2013)* proposed a southward dispersal for *H. habilis*, which we could not identify in our study. Overall, our result suggests that range expansion dispersals happened more frequently than previously suggested (*Strait, 2013*). The pattern of dispersals found in our study also contradicts previous findings on dispersal asymmetry in early hominins by *Strait and Wood (1999)* and *Strait (2013)*. Importantly, neither *Strait and Wood (1999)* nor *Strait (2013)* included *A. sediba* in their studies.

## 5. Conclusions

Historical biogeography has moved away from estimating patterns of species distribution to incorporating biogeographical processes. Here, we examined biogeographical processes shaping hominin distribution within Africa. The result of this study suggested that Northcentral Africa and eastern Africa<sub>North</sub> and Middle were the centers of origin for multiple early taxa. For the rest of the ancestral nodes, a tree in which *A. sediba* and *A. africanus* are sister taxa inferred widespread ancestors in eastern Africa<sub>North</sub> and Middle and southern Africa or eastern Africa<sub>Middle</sub> and southern Africa. However, a tree in which *A. sediba* is the sister taxon of *Homo* inferred endemic ancestors in eastern Africa<sub>North</sub>, eastern Africa<sub>Middle</sub>, or southern Africa. Further efforts to resolve the phylogenetic relationships of *A. sediba* should therefore have important implications for our understanding of hominin biogeography and, by extension, paleobiology. Our results suggest that sympatry, dispersal, and extinction were major biogeographical processes in early hominin evolution. In contrast, founder events and, particularly, vicariance were not as common. While some of our results were robust in both trees, others differed based on the choice of the phylogenetic tree. Unlike the parsimony approach used in previous studies, probabilistic biogeographical approaches incorporate information about branch lengths and quantify the likelihood of inferred results. Both are critical in studying macroevolutionary processes and need to be incorporated into biogeographical studies.

## CRediT authorship contribution statement

**Yeganeh Sekhavati:** Writing – original draft, Visualization, Methodology, Funding acquisition, Formal analysis, Data curation, Conceptualization. **David Strait:** Writing – review & editing, Supervision, Funding acquisition, Conceptualization.

## Acknowledgments

We are grateful to Michael Landis and Rich Smith for insightful comments. This research was funded by the Wenner-Gren Foundation (Gr. 10244) and the Biological Anthropology Directorate of the National Science Foundation (BCS-2141883).

## Supplementary Online Material

Supplementary Online Material related to this article can be found at <https://doi.org/10.1016/j.jhevol.2024.103547>.

## References

- Asfaw, B., 1987. The Belohdelie frontal: New evidence of early hominid cranial morphology from the Afar of Ethiopia. *J. Hum. Evol.* 16, 611–624. [https://doi.org/10.1016/0047-2484\(87\)90016-9](https://doi.org/10.1016/0047-2484(87)90016-9).
- Asfaw, B., White, T., Lovejoy, O., Latimer, B., Simpson, S., Suwa, G., 1999. *Australopithecus garhi*: A new species of early hominid from Ethiopia. *Science* 284, 629–635. <https://doi.org/10.1126/science.284.5414.629>.
- Bapst, D.W., 2012. paleotree: An R package for paleontological and phylogenetic analyses of evolution. *Methods Ecol. Evol.* 3, 803–807. <https://doi.org/10.1111/j.2041-210X.2012.00223.x>.
- Behrensmeyer, A.K., Reed, K.E., 2013. Reconstructing the habitats of *Australopithecus*: Paleoenvironments, site taphonomy, and faunas. In: Reed, K.E., Fleagle, J.G., Leakey, R.E. (Eds.), *The Paleobiology of Australopithecus*. Springer, Dordrecht, pp. 41–60. [https://doi.org/10.1007/978-94-007-5919-0\\_4](https://doi.org/10.1007/978-94-007-5919-0_4).
- Berger, B.A., Kriebel, R., Spalink, D., Sytsma, K.J., 2016. Divergence times, historical biogeography, and shifts in speciation rates of Myrtales. *Mol. Phylogenetic Evol.* 95, 116–136. <https://doi.org/10.1016/j.ympev.2015.10.001>.
- Berger, L.R., De Ruiter, D.J., Churchill, S.E., Schmid, P., Carlson, K.J., Dirks, P.H., Kibii, J.M., 2010. *Australopithecus sediba*: A new species of *Homo*-like Australopith from South Africa. *Science* 328, 195–204. <https://doi.org/10.1126/science.1184944>.
- Boles, O.J., Shoemaker, A., Courtney Mustaphi, C.J., Petek, N., Ekblom, A., Lane, P.J., 2019. Historical ecologies of pastoralist overgrazing in Kenya: Long-term perspectives on cause and effect. *Hum. Ecol.* 47, 419–434. <https://doi.org/10.1007/s10745-019-0072-9>.
- Bollback, J.P., 2006. SIMMAP: Stochastic character mapping of discrete traits on phylogenies. *MCB Bioinf.* 7, 1–7. <https://doi.org/10.1186/1471-2105-7-88>.
- Bremer, K., 1992. Ancestral areas: A cladistic reinterpretation of the center of origin concept. *Syst. Biol.* 41, 436–445. <https://doi.org/10.1093/sysbio/41.4.436>.
- Bremer, K., 1995. Ancestral areas: Optimization and probability. *Syst. Biol.* 44, 255–259. <https://doi.org/10.2307/2413711>.
- Brocklehurst, N., 2016. Rates and modes of body size evolution in early carnivores and herbivores: A case study from Captorhinidae. *PeerJ* 4, e1555. <https://doi.org/10.7717/peerj.1555>.
- Bromage, T.G., Schrenk, F., 1995. Biogeographic and climatic basis for a narrative of early hominid evolution. *J. Hum. Evol.* 28, 109–114. <https://doi.org/10.1006/jhev.1995.1008>.
- Brown, F.H., McDougall, I., Gathogo, P.N., 2013. Age ranges of *Australopithecus* species, Kenya, Ethiopia, and Tanzania. In: Reed, K.E., Fleagle, J.G., Leakey, R.E. (Eds.), *The Paleobiology of Australopithecus*. Springer, Dordrecht, pp. 7–20. [https://doi.org/10.1007/978-94-007-5919-0\\_2](https://doi.org/10.1007/978-94-007-5919-0_2).
- Brunet, M., Beauvilain, A., Coppens, Y., Heintz, E., Moutaye, A.H., Pilbeam, D., 1995. The first australopithecine 2,500 kilometres west of the Rift Valley (Chad). *Nature* 378, 273–275. <https://doi.org/10.1038/378273a0>.
- Buerki, S., Forest, F., Alvarez, N., Nylander, J.A.A., Arrigo, N., Sanmartín, I., 2011. An evaluation of new parsimony-based versus parametric inference methods in biogeography: A case study using the globally distributed plant family Sapindaceae. *J. Biogeogr.* 38, 531–550. <https://doi.org/10.1111/j.1365-2699.2010.02432.x>.
- Burnham, K.P., Anderson, D.R., 2002. *Model Selection and Multimodel Inference*, second ed. Springer, New York.
- Carotenuto, F., Tsikaridze, N., Rook, L., Lordkipanidze, D., Longo, L., Condemi, S., Raia, P., 2016. Venturing out safely: The biogeography of *Homo erectus* dispersal out of Africa. *J. Hum. Evol.* 95, 1–12. <https://doi.org/10.1016/j.jhevol.2016.02.005>.

Caswell, J.L., Mallick, S., Richter, D.J., Neubauer, J., Schirmer, C., Gnerre, S., Reich, D., 2008. Analysis of chimpanzee history based on genome sequence alignments. *PLoS Genet.* 4, e1000057. <https://doi.org/10.1371/journal.pgen.1000057>.

Clarke, R.J., Kuman, K., 2019. The skull of StW 573, a 3.67 Ma *Australopithecus prometheus* skeleton from Sterkfontein Caves, South Africa. *J. Hum. Evol.* 134, 102634. <https://doi.org/10.1016/j.jhevol.2019.06.005>.

Cox, B., 2001. The biogeographic regions reconsidered. *J. Biogeogr.* 28, 511–523. <https://doi.org/10.1046/j.jbiogeo.2000.00566.x>.

Cox, B., 2010. Underpinning global biogeographical schemes with quantitative data. *J. Biogeogr.* 37, 2027–2028. <https://doi.org/10.1111/j.1365-2699.2010.02420.x>.

Crisci, J.V., Sala, O.E., Katinas, L., Posadas, P., 2006. Bridging historical and ecological approaches in biogeography. *Aust. Syst. Bot.* 19, 1–10. <https://doi.org/10.1071/SB05006>.

Crisp, M.D., Trewick, S.A., Cook, L.G., 2011a. Hypothesis testing in biogeography. *Trends Ecol. Evol.* 26, 66–72. <https://doi.org/10.1016/j.tree.2010.11.005>.

Crisp, M.D., Trewick, S.A., Cook, L.G., 2011b. Hypothesis testing in biogeography. *Trends Ecol. Evol.* 26, 66–72. <https://doi.org/10.1016/j.tree.2010.11.005>.

Cuthbert, M.O., Gleeson, T., Reynolds, S.C., Bennett, M.R., Newton, A.C., McCormack, C.J., Ashley, G.M., 2017. Modelling the role of groundwater hydro-refugia in East African hominin evolution and dispersal. *Nat. Commun.* 8, 1–11. <https://doi.org/10.1038/ncomms15696>.

De Manuel, M., Kuhlwilm, M., Frandsen, P., Sousa, V.C., Desai, T., Prado-Martinez, J., Hernandez-Rodriguez, J., Dupanloup, I., Lao, O., Hallast, P., 2016. Chimpanzee genomic diversity reveals ancient admixture with bonobos. *Science* 354, 477–481. <https://doi.org/10.1126/science.aag2602>.

de Queiroz, K., 1998. The general lineage concept of species, species criteria, and the process of speciation. A conceptual unification and terminological recommendations. In: Howard, D.J., Berlocher, S.H. (Eds.), *Endless Forms: Species and Speciation*. Oxford University Press, Oxford, pp. 57–75.

de Queiroz, K., 2007. Species concepts and species delimitation. *Syst. Biol.* 56, 879–886.

Deino, A.L., 2011. 40 Ar/39 Ar dating of Laetoli, Tanzania. In: Harrison, T. (Ed.), *Paleontology and Geology of Laetoli: Human Evolution in Context*. Springer, Dordrecht, pp. 77–97. [https://doi.org/10.1007/978-90-481-9956-3\\_4](https://doi.org/10.1007/978-90-481-9956-3_4).

Delson, E., 1986. Palaeoanthropology: Human phylogeny revised again. *Nature* 322, 496–497. <https://doi.org/10.1038/322496b0>.

Dennell, R.W., Louys, J., O'Regan, H.J., Wilkinson, D.M., 2014. The origins and persistence of *Homo floresiensis* on Flores: Biogeographical and ecological perspectives. *Quat. Sci. Rev.* 96, 98–107. <https://doi.org/10.1016/j.quascirev.2013.06.031>.

Dominguez-Rodrigo, M., Pickering, T.R., Baquedano, E., Mabulla, A., Mark, D.F., Musiba, C., Bunn, H.T., Uribelarrea, D., Smith, V., Diez-Martin, F., Perez-Gonzalez, A., Sanchez, P., Santonja, M., Barbón, D., Gidna, A., Ashley, G., Yravedra, J., Heaton, J.L., Arriaza, M.C., 2013. First partial skeleton of a 1.34-million-year-old *Paranthropus boisei* from Bed II, Olduvai Gorge, Tanzania. *PLoS One* 8, e80347. <https://doi.org/10.1371/journal.pone.0080347>.

Dupin, J., Matzke, N.J., Särkinen, T., Knapp, S., Olmstead, R.G., Bohs, L., Smith, S.D., 2017. Bayesian estimation of the global biogeographical history of the Solanaceae. *J. Biogeogr.* 44, 887–899. <https://doi.org/10.1111/jbi.12898>.

Eichhorn, M.P., Baker, K., Griffiths, M., 2020. Steps towards decolonising biogeography. *Front. Biogeogr.* 12. <https://doi.org/10.21425/F5FBG44795>.

Escalante, T., Morrone, J.J., Rodríguez-Tapia, G., 2013. Biogeographic regions of North American mammals based on endemism. *Biol. J. Linn. Soc.* 110, 485–499. <https://doi.org/10.1111/bj.12142>.

Faith, J.T., Du, A., Behrensmeyer, A.K., Davies, B., Patterson, D.B., Rowan, J., Wood, B., 2021. Rethinking the ecological drivers of hominin evolution. *Trends Ecol. Evol.* 36, 797–807. <https://doi.org/10.1016/j.tree.2021.04.011>.

Fattorini, S., 2017. Endemism in historical biogeography and conservation biology: Concepts and implications. *Biogeographia* 32. <https://doi.org/10.21426/B632136433>.

Fauby, S., Svensson, J.C., 2015. Historic and prehistoric human-driven extinctions have reshaped global mammal diversity patterns. *Divers. Distrib.* 21, 1155–1166. <https://doi.org/10.1111/ddi.12369>.

Feibel, C.S., Brown, F.H., McDougall, I., 1989. Stratigraphic context of fossil hominids from the Omo Group deposits: Northern Turkana Basin, Kenya and Ethiopia. *Am. J. Phys. Anthropol.* 78, 595–622. <https://doi.org/10.1002/ajpa.1330780412>.

Foley, R., 2003. Adaptive radiations and dispersals in hominin evolutionary ecology. *Evol. Anthropol.* 11, 32–37. <https://doi.org/10.1002/evan.10051>.

Foley, R.A., 2013. Comparative evolutionary models and the "Australopith Radiations". In: Reed, K.E., Fleagle, J.G., Leakey, R.E. (Eds.), *The Paleobiology of Australopithecus*. Springer, Dordrecht, pp. 163–174. [https://doi.org/10.1007/978-94-007-5919-0\\_10](https://doi.org/10.1007/978-94-007-5919-0_10).

Foley, R.A., 2018. Evolutionary geography and the Afro-tropical model of hominin evolution. *Bull. Mém. Soc. Anthropol.* Paris 30, 17–31. <https://doi.org/10.3166/bmsap-2018-0001>.

Folk, R.A., Visger, C.J., Soltis, P.S., Soltis, D.E., Guralnick, R.P., 2018. Geographic range dynamics drove ancient hybridization in a lineage of angiosperms. *Am. Nat.* 192, 171–187. <https://doi.org/10.5061/dryad.7cr0c76>.

Gathogo, P.N., Brown, F.H., 2006. Revised stratigraphy of Area 123, Koobi Fora, Kenya, and new age estimates of its fossil mammals, including hominins. *J. Hum. Evol.* 51, 471–479. <https://doi.org/10.1016/j.jhevol.2006.05.005>.

Gibbon, R.J., Pickering, T.R., Sutton, M.B., Heaton, J.L., Kuman, K., Clarke, R.J., Brain, C., Granger, D.E., 2014. Cosmogenic nuclide burial dating of hominin-bearing Pleistocene cave deposits at Swartkrans, South Africa. *Quat. Geochronol.* 24, 10–15. <https://doi.org/10.1016/j.quageo.2014.07.004>.

Grine, F.E., 1988. *Evolutionary History of the Robust Australopithecines*. Aldine de Gruyter, New York.

Grine, F.E., 1989. New hominid fossils from the Swartkrans Formation (1979–1986 excavations): Craniodental specimens. *Am. J. Phys. Anthropol.* 79, 409–449. <https://doi.org/10.1002/ajpa.1330790402>.

Haile-Selassie, Y., Melillo, S.M., 2015. Middle Pliocene hominin mandibular fourth premolars from Woranso-Mille (central Afar, Ethiopia). *J. Hum. Evol.* 78, 44–59. <https://doi.org/10.1016/j.jhevol.2014.08.005>.

Haile-Selassie, Y., Melillo, S.M., Su, D.F., 2016. The Pliocene hominin diversity conundrum: Do more fossils mean less clarity? *Proc. Natl. Acad. Sci. USA* 113, 6364–6371. <https://doi.org/10.1073/pnas.1521266113>.

Haile-Selassie, Y., Saylor, B.Z., Deino, A., Alene, M., Latimer, B.M., 2010. New hominid fossils from Woranso-Mille (central Afar, Ethiopia) and taxonomy of early *Australopithecus*. *Am. J. Phys. Anthropol.* 141, 406–417. <https://doi.org/10.1002/ajpa.21159>.

Harrison, T., 2002. The first record of fossil hominins from the Ndalanya Beds, Laetoli, Tanzania. *Am. J. Phys. Anthropol.* 32, 83.

Harrison, T., 2011. Hominins from the upper Laetolil and upper Ndalanya beds, Laetoli. In: Harrison, T. (Ed.), *Paleontology and Geology of Laetoli: Human Evolution in Context*. Springer, Dordrecht, pp. 141–188. [https://doi.org/10.1007/978-90-481-9962-4\\_7](https://doi.org/10.1007/978-90-481-9962-4_7).

He, J., Kreft, H., Gao, E., Wang, Z., Jiang, H., 2017. Patterns and drivers of zoogeographical regions of terrestrial vertebrates in China. *J. Biogeogr.* 44, 1172–1184. <https://doi.org/10.1111/jbi.12892>.

Heinzelin, J.D., Clark, J.D., White, T., Hart, W., Renne, P., WoldeGabriel, G., Beyene, Y., Vrba, E., 1999. Environment and behavior of 2.5-million-year-old Bouri hominids. *Science* 284, 625–629. <https://doi.org/10.1126/science.284.5414.625>.

Herries, A.I., Martin, J.M., Leece, A., Adams, J.W., Boschian, G., Joannes-Boyau, R., Edwards, T.R., Mallett, T., Massey, J., Murszewski, A., 2020. Contemporaneity of *Australopithecus*, *Paranthropus*, and early *Homo erectus* in South Africa. *Science* 368, eaaw7293. <https://doi.org/10.1126/science.aaw7293>.

Herries, A.I., Pickering, R., Adams, J.W., Curnoe, D., Warr, G., Latham, A.G., Shaw, J., 2013. A multi-disciplinary perspective on the age of *Australopithecus* in southern Africa. In: Reed, K.E., Fleagle, J.G., Leakey, R.E. (Eds.), *The Paleobiology of Australopithecus*. Springer, Dordrecht, pp. 21–40. [https://doi.org/10.1007/978-94-007-5919-0\\_3](https://doi.org/10.1007/978-94-007-5919-0_3).

Huelsenbeck, J.P., Nielsen, R., Bollback, J.P., 2003. Stochastic mapping of morphological characters. *Syst. Biol.* 52, 131–158. <https://doi.org/10.1080/10635150390192780>.

Hunt, G., 2013. Testing the link between phenotypic evolution and speciation: An integrated palaeontological and phylogenetic analysis. *Methods Ecol. Evol.* 4, 714–723. <https://doi.org/10.1111/2041-210X.12085>.

Hunt, G., Carrano, M.T., 2010. Models and methods for analyzing phenotypic evolution in lineages and clades. *Paleontol. Soc. Pap.* 16, 245–269. <https://doi.org/10.1017/S108932600001893>.

Irish, J.D., Guatelli-Steinberg, D., Legge, S.S., de Ruiter, D.J., Berger, L.R., 2013. Dental morphology and the phylogenetic "place" of *Australopithecus sediba*. *Science* 340, 1233062. <https://doi.org/10.1126/science.1233062>.

Joordens, J.C.A., Feibel, C.S., Vonhof, H.B., Schulp, A.S., Kroon, D., 2019. Relevance of the eastern African coastal forest for early hominin biogeography. *J. Hum. Evol.* 131, 176–202. <https://doi.org/10.1016/j.jhevol.2019.03.012>.

Kier, G., Kreft, H., Lee, T.M., Jetz, W., Ibischi, P.L., Nowicki, C., Mutke, J., Barthlott, W., 2009. A global assessment of endemism and species richness across island and mainland regions. *Proc. Natl. Acad. Sci. USA* 106, 9322–9327. <https://doi.org/10.1073/pnas.0810306106>.

Kimbrel, W.H., Delezenne, L.K., 2009. "Lucy" redux: A review of research on *Australopithecus afarensis*. *Am. J. Phys. Anthropol.* 140 (Suppl. 49), 2–48. <https://doi.org/10.1002/ajpa.21183>.

Kimbrel, W.H., Johanson, D.C., Rak, Y., 1994. The first skull and other new discoveries of *Australopithecus afarensis* at Hadar, Ethiopia. *Nature* 368, 449–451. <https://doi.org/10.1038/368449a0>.

Kimbrel, W.H., Rak, Y., 2017. *Australopithecus sediba* and the emergence of *Homo*: Questionable evidence from the cranium of the juvenile holotype MH 1. *J. Hum. Evol.* 107, 94–106. <https://doi.org/10.1016/j.jhevol.2017.03.011>.

Kimbrel, W.H., Walter, R.C., Johanson, D.C., Reed, K.E., Aronson, J.L., Assefa, Z., Marean, C.W., Eck, G., Bobe, R., Hovers, E., 1996. Late Pliocene *Homo* and Oldowan tools from the Hadar Formation (Kada Hadar Member), Ethiopia. *J. Hum. Evol.* 31, 549–561. <https://doi.org/10.1006/jhev.1996.0079>.

Kodandaramaiah, U., 2010. Use of dispersal-vicariance analysis in biogeography – A critique. *J. Biogeogr.* 37, 3–11. <https://doi.org/10.1111/j.1365-2699.2009.02221.x>.

Kreft, H., Jetz, W., 2010. A framework for delineating biogeographical regions based on species distributions. *J. Biogeogr.* 37, 2029–2053. <https://doi.org/10.1111/j.1365-2699.2010.02375.x>.

Kuhlwilm, M., Han, S., Sousa, V.C., Excoffier, L., Marques-Bonet, T., 2019. Ancient admixture from an extinct ape lineage into bonobos. *Nat. Ecol. Evol.* 3, 957–965. <https://doi.org/10.1038/s41559-019-0881-7>.

Kullmer, O., Sandrock, O., Abel, R., Schrenk, F., Bromage, T.G., Juwayeyi, Y.M., 1999. The first *Paranthropus* from the Malawi rift. *J. Hum. Evol.* 37, 121–127. <https://doi.org/10.1006/jhev.1999.0308>.

Kuman, K., Granger, D.E., Gibbon, R.J., Pickering, T.R., Caruana, M.V., Bruxelles, L., Clarke, R.J., Heaton, J.L., Stratford, D., Brain, C., 2021. A new absolute date from Swartkrans Cave for the oldest occurrences of *Paranthropus robustus* and Oldowan stone tools in South Africa. *J. Hum. Evol.* 156, 103000. <https://doi.org/10.1016/j.jhevol.2021.103000>.

Lahr, M.M., Foley, R., 1994. Multiple dispersals and modern human origins. *Evol. Anthropol.* 3, 48–60. <https://doi.org/10.1002/evan.1360030206>.

Lamm, K.S., Redelings, B.D., 2009. Reconstructing ancestral ranges in historical biogeography: Properties and prospects. *J. Syst. Evol.* 47, 369–382. <https://doi.org/10.1111/j.1759-6831.2009.00042.x>.

Landis, M.J., Matzke, N.J., Moore, B.R., Hulsenbeck, J.P., 2013. Bayesian analysis of biogeography when the number of areas is large. *Syst. Biol.* 62, 789–804. <https://doi.org/10.1093/sysbio/syt040>.

Leakey, M.G., Feibel, C.S., McDougall, I., Walker, A., 1995. New four-million-year-old hominid species from Kanapoi and Allia Bay, Kenya. *Nature* 376, 565–571. <https://doi.org/10.1038/376565a0>.

Lebatard, A.-E., Bourlès, D.L., Duringer, P., Jolivet, M., Braucher, R., Carcaillet, J., Schuster, M., Arnaud, N., Monié, P., Lihoreau, F., 2008. Cosmogenic nuclide dating of *Sahelanthropus tchadensis* and *Australopithecus bahrelghazali*: Miocene hominids from Chad. *Proc. Natl. Acad. Sci. USA* 105, 3226–3231. <https://doi.org/10.1073/pnas.0708015105>.

Lieberman, B.S., 2002. Phylogenetic biogeography with and without the fossil record: Gauging the effects of extinction and paleontological incompleteness. *Palaeogeogr. Palaeoclimatol. Palaeoecol.* 178, 39–52. [https://doi.org/10.1016/S0030-0182\(01\)00367-4](https://doi.org/10.1016/S0030-0182(01)00367-4).

Linder, H.P., de Klerk, H.M., Born, J., Burgess, N.D., Fjeldså, J., Rahbek, C., 2012. The partitioning of Africa: Statistically defined biogeographical regions in sub-Saharan Africa. *J. Biogeogr.* 39, 1189–1205. <https://doi.org/10.1111/j.1365-2699.2012.02728.x>.

Macho, G.A., 2015. Pliocene hominin biogeography and ecology. *J. Hum. Evol.* 87, 78–86. <https://doi.org/10.1016/j.jhevol.2015.06.009>.

Macho, G.A., 2017. Niche partitioning. In: Fuentes, A. (Ed.), *The International Encyclopedia of Primatology*. Wiley-Blackwell, Hoboken. <https://doi.org/10.1002/9781119179313.wbprim0366>.

Mailund, T., Halager, A.E., Westergaard, M., Dutheil, J.Y., Munch, K., Andersen, L.N., Lunter, G., Pruffer, K., Scally, A., Hobolth, A., Schierup, M.H., 2012. A new isolation with migration model along complete genomes infers very different divergence processes among closely related great ape species. *PLoS Genet.* 8, e1003125. <https://doi.org/10.1371/journal.pgen.1003125>.

Martin, J.M., Leece, A.B., Baker, S., Herries, A.I.R., Strait, D.S., 2024. A lineage perspective on hominin taxonomy and evolution. *Evol. Anthropol.* 33, e22018.

Martin, J.M., Leece, A., Neubauer, S., Baker, S.E., Monge, C.S., Boschian, G., Schwartz, G.T., Smith, A.L., Ledogar, J.A., Strait, D.S., 2021. Drimolen cranium DNH 155 documents microevolution in an early hominin species. *Nat. Ecol. Evol.* 5, 38–45. <https://doi.org/10.1038/s41559-020-01319-6>.

Massana, K.A., Beaulieu, J.M., Matzke, N.J., O'Meara, B.C., 2015. Non-null effects of the null range in biogeographic models: Exploring parameter estimation in the DEC model. *BioRxiv* preprint available at: <https://doi.org/10.1101/026914>. (Accessed 15 August 2021).

Mateo, R.G., Vanderpoorten, A., Muñoz, J., Laenen, B., Désamoré, A., 2013. Modeling species distributions from heterogeneous data for the biogeographic regionalization of the European bryophyte flora. *PLoS One* 8, e55648. <https://doi.org/10.1371/journal.pone.0055648>.

Matzke, N.J., 2013. Probabilistic historical biogeography: New models for founder-event speciation, imperfect detection, and fossils allow improved accuracy and model-testing. *Front. Biogeogr.* 5. <https://doi.org/10.21425/f5fbg19694>.

Matzke, N.J., 2014. Model selection in historical biogeography reveals that founder-event speciation is a crucial process in island clades. *Syst. Biol.* 63, 951–970. <https://doi.org/10.1093/sysbio/syu056>.

Maxwell, S.J., Hopley, P.J., Upchurch, P., Soligo, C., 2018. Sporadic sampling, not climatic forcing, drives observed early hominin diversity. *Proc. Natl. Acad. Sci. USA* 115, 4891–4896. <https://doi.org/10.1073/pnas.1721538115>.

Mayer, E., 1954. *Change of genetic environment and evolution*. In: Huxley, J., Hardy, A.C., Ford, E.B. (Eds.), *Evolution as a Process*. Allen and Unwin, London, pp. 157–180.

McDougall, I., Brown, F.H., 2006. Precise  $^{40}\text{Ar}/^{39}\text{Ar}$  geochronology for the upper Koobi Fora Formation, Turkana Basin, northern Kenya. *J. Geol. Soc.* 163, 205–220. <https://doi.org/10.1144/0016-764904-166>.

McDougall, I., Brown, F.H., 2008. Geochronology of the pre-KBS tuff sequence, Omo Group, Turkana Basin. *J. Geol. Soc.* 165, 549–562. <https://doi.org/10.1144/0016-76492006-170>.

McDougall, I., Brown, F.H., Vasconcelos, P.M., Cohen, B.E., Thiede, D.S., Buchanan, M.J., 2012. New single crystal  $^{40}\text{Ar}/^{39}\text{Ar}$  ages improve time scale for deposition of the Omo Group, Omo–Turkana Basin, East Africa. *J. Geol. Soc.* 169, 213–226. <https://doi.org/10.1144/0016-76492010-188>.

McDowall, R., 2004. What biogeography is: A place for process. *J. Biogeogr.* 31, 345–351.

McFadden, P., Brock, A., Partridge, T., 1979. Palaeomagnetism and the age of the Makapansgat hominid site. *Earth Planet. Sci. Lett.* 44, 373–382. [https://doi.org/10.1016/0012-821X\(79\)90076-1](https://doi.org/10.1016/0012-821X(79)90076-1).

Monarrez, P.M., Zimmt, J.B., Clement, A.M., Gearty, W., Jacisin, J.J., Jenkins, K.M., Kusnerik, K.M., Poust, A.W., Robson, S.V., Sclafani, J.A., 2022. Our past creates our present: A brief overview of racism and colonialism in Western paleontology. *Paleobiology* 48, 173–185. <https://doi.org/10.1017/pab.2021.28>.

Mondanaro, A., Melchionna, M., Di Febbraro, M., Castiglione, S., Holden, P.B., Edwards, N.R., Carotenuto, F., Maiorano, L., Modafferi, M., Serio, C., 2020. A major change in rate of climate niche envelope evolution during hominid history. *iScience* 23, 101693. <https://doi.org/10.1016/j.isci.2020.101693>.

Monge, C.S., Pugh, K.D., Strait, D.S., Grine, F.E., 2022. Modelling hominin evolution requires accurate hominin data. *Nat. Ecol. Evol.* 6, 1090–1091. <https://doi.org/10.1038/s41559-022-01791-2>.

Monge, C.S., Strait, D.S., Grine, F.E., 2019. Expanded character sampling underscores phylogenetic stability of *Ardipithecus ramidus* as a basal hominin. *J. Hum. Evol.* 131, 28–39. <https://doi.org/10.1016/j.jhevol.2019.03.006>.

Monge, C.S., Strait, D.S., Grine, F.E., 2023. An updated analysis of hominin phylogeny with an emphasis on re-evaluating the phylogenetic relationships of *Australopithecus sediba*. *J. Hum. Evol.* 175, 103311. <https://doi.org/10.1016/j.jhevol.2022.103311>.

Moorjani, P., Amorim, C.E.G., Arndt, P.F., Przeworski, M., 2016. Variation in the molecular clock of primates. *Proc. Natl. Acad. Sci. USA* 113, 10607–10612. <https://doi.org/10.1073/pnas.1600374113>.

Morrone, J.J., 1994. On the identification of areas of endemism. *Syst. Biol.* 43, 438–441. <https://doi.org/10.1093/sysbio/43.3.438>.

Morrone, J.J., 2015. Biogeographical regionalisation of the world: A reappraisal. *Aust. Syst. Bot.* 28, 81–90. <https://doi.org/10.1071/SB14042>.

Morrone, J.J., 2018. The spectre of biogeographical regionalization. *J. Biogeogr.* 45, 282–288. <https://doi.org/10.1111/jbi.13135>.

Morrone, J.J., Crisci, J.V., 1995. Historical biogeography: Introduction to methods. *Ann. Rev. Ecol. Syst.* 26, 373–401. <https://doi.org/10.1146/annurev.es.26.110195.002105>.

Murguía, M., Llorente-Bousquet, J., 2003. *Reflexiones Conceptuales en Biogeografía Cuantitativa. Una Perspectiva Latinoamericana de la Biogeografía*. Las Prensas de Ciencias. Facultad de Ciencias UNAM, México.

Naranjo, A.A., Folk, R.A., Gitzendanner, M.A., Soltis, D.E., Soltis, P.S., 2023. Ancestral area analyses reveal Pleistocene-influenced evolution in a clade of coastal plain endemic plants. *J. Biogeogr.* 50, 393–405. <https://doi.org/10.1111/jbi.14541>.

Nielsen, R., 2002. Mapping mutations on phylogenies. *Syst. Biol.* 51, 729–739. <https://doi.org/10.1080/10635150290102393>.

Partridge, T., Latham, A., Heslop, D., 2000. Appendix on magnetostratigraphy of Makapansgat, Sterkfontein, Taung and Swartkrans. In: Partridge, T.C., Maud, R.R. (Eds.), *The Cenozoic of Southern Africa*. Oxford Monographs on Geology and Geophysics. Oxford University Press, Oxford, pp. 126–129.

Patterson, N., Richter, D.J., Gnerre, S., Lander, E.S., Reich, D., 2006. Genetic evidence for complex speciation of humans and chimpanzees. *Nature* 441, 1103–1108. <https://doi.org/10.1038/nature04789>.

Pickering, R., Dirks, P.H., Jinnah, Z., De Ruiter, D.J., Churchill, S.E., Herries, A.I., Woodhead, J.D., Hellstrom, J.C., Berger, L.R., 2011a. *Australopithecus sediba* at 1.977 Ma and implications for the origins of the genus *Homo*. *Science* 333, 1421–1423. <https://doi.org/10.1126/science.1203697>.

Pickering, R., Kramers, J.D., Hancox, P.J., de Ruiter, D.J., Woodhead, J.D., 2011b. Contemporary flowstone development links early hominin bearing cave deposits in South Africa. *Earth Planet. Sci. Lett.* 306, 23–32. <https://doi.org/10.1016/j.epsl.2011.03.019>.

Pickering, R., Herries, A.I., 2020. A new multidisciplinary age of 2.61–2.07 Ma for the Sterkfontein Member 4 australopiths. In: Zipfel, B., Richmond, B.G., Ward, C.V. (Eds.), *Hominin Postcranial Remains from Sterkfontein, South Africa, 1936–1995*. Oxford University Press, Oxford, pp. 21–30. <https://doi.org/10.1093/oso/9780197507667.003.0003>.

Popper, K., 2005. *The Logic of Scientific Discovery*. Routledge, London.

Potts, R., Behrensmeyer, A.K., Deino, A., Ditchfield, P., Clark, J., 2004. Small mid-Pleistocene hominin associated with East African Acheulean technology. *Science* 305, 75–78. <https://doi.org/10.1126/science.1097661>.

Raia, P., Mondanaro, A., Melchionna, M., Di Febbraro, M., Diniz-Filho, J.A., Rangel, T.F., Holden, P.B., Carotenuto, F., Edwards, N.R., Lima-Ribeiro, M.S., 2020. Past extinctions of *Homo* species coincided with increased vulnerability to climatic change. *One Earth* 3, 480–490. <https://doi.org/10.1016/j.oneear.2020.09.007>.

Raja, N.B., Dunne, E.M., Matiwane, A., Khan, T.M., Näscher, P.S., Ghilardi, A.M., Chattopadhyay, D., 2022. Colonial history and global economics distort our understanding of deep-time biodiversity. *Nat. Ecol. Evol.* 6, 145–154. <https://doi.org/10.1038/OSI.10/6WC7A>.

Ree, R.H., 2005. Detecting the historical signature of key innovations using stochastic models of character evolution and cladogenesis. *Evolution* 59, 257–265. <https://doi.org/10.1111/j.0014-3820.2005.tb00986.x>.

Ree, R.H., Moore, B.R., Webb, C.O., Donoghue, M.J., 2005. A likelihood framework for inferring the evolution of geographic range on phylogenetic trees. *Evolution* 59, 2299–2311. <https://doi.org/10.1111/j.0014-3820.2005.tb00940.x>.

Ree, R.H., Sanmartín, I., 2018. Conceptual and statistical problems with the DEC+ J model of founder-event speciation and its comparison with DEC via model selection. *J. Biogeogr.* 45, 741–749. <https://doi.org/10.1111/jbi.13173>.

Ree, R.H., Smith, S.A., 2008. Maximum likelihood inference of geographic range evolution by dispersal, local extinction, and cladogenesis. *Syst. Biol.* 57, 4–14. <https://doi.org/10.1080/10635150701883881>.

Ronquist, F., 1995. Reconstructing the history of host-parasite associations using generalised parsimony. *Cladistics* 11, 73–89. <https://doi.org/10.1111/j.1096-0031.1995.tb00005.x>.

Ronquist, F., 1997. Dispersal-vicariance analysis: A new approach to the quantification of historical biogeography. *Syst. Biol.* 46, 195–203. <https://doi.org/10.1093/sysbio/46.1.195>.

Ronquist, F., Sanmartín, I., 2011. Phylogenetic methods in biogeography. *Ann. Rev. Ecol. Evol. Syst.* 42, 441–464. <https://doi.org/10.1146/annurev-ecolsys-102209-144710>.

Sanmartín, I., Ronquist, F., 2004. Southern hemisphere biogeography inferred by event-based models: Plant versus animal patterns. *Syst. Biol.* 53, 216–243. <https://doi.org/10.1080/10635150490423430>.

Scally, A., Dutheil, J.Y., Hillier, L.W., Jordan, G.E., Goodhead, I., Herrero, J., Hobolth, A., Lappalainen, T., Mailund, T., Marques-Bonet, T., 2012. Insights into hominid evolution from the gorilla genome sequence. *Nature* 483, 169–175.

Scerri, E.M., Thomas, M.G., Manica, A., Gunz, P., Stock, J.T., Stringer, C., Grove, M., Groucutt, H.S., Timmermann, A., Rightmire, G.P., 2018. Did our species evolve in subdivided populations across Africa, and why does it matter? *Trends Ecol. Evol.* 33, 582–594. <https://doi.org/10.1016/j.tree.2018.05.005>.

Schroer, K., Wood, B., 2015. The role of character displacement in the polarization of hominin mandibular premolars. *Evolution* 69, 1630–1642. <https://doi.org/10.1111/evol.12672>.

Semaw, S., Simpson, S.W., Quade, J., Renne, P.R., Butler, R.F., McIntosh, W.C., Levin, N., Dominguez-Rodrigo, M., Rogers, M.J., 2005. Early Pliocene hominids from Gona, Ethiopia. *Nature* 433, 301–305. <https://doi.org/10.1038/nature03177>.

Simpson, S.W., Levin, N.E., Quade, J., Rogers, M.J., Semaw, S., 2019. *Ardipithecus ramidus* postcrania from the Gona Project area, Afar Regional State, Ethiopia. *J. Hum. Evol.* 129, 1–45. <https://doi.org/10.1016/j.jhevol.2018.12.005>.

Sinclair, A.R., Packer, C., Mduma, S.A., Fryxell, J.M., 2009. *Serengeti III: Human Impacts on Ecosystem Dynamics*. University of Chicago Press, Chicago.

Skelton, R.R., McHenry, H.M., 1992. Evolutionary relationships among early hominids. *J. Hum. Evol.* 23, 309–349. [https://doi.org/10.1016/0047-2484\(92\)90070-P](https://doi.org/10.1016/0047-2484(92)90070-P).

Soto-Trejo, F., Matzke, N.J., Schilling, E.E., Massana, K.A., Oyama, K., Lira, R., Dávila, P., 2017. Historical biogeography of Florestina (Asteraceae: Bahieae) of dry environments in Mexico: Evaluating models and uncertainty in low-diversity clades. *Bot. J. Linn. Soc.* 185, 497–510. <https://doi.org/10.1093/botlinean/box069>.

Soul, L.C., Friedman, M., 2015. Taxonomy and phylogeny can yield comparable results in comparative paleontological analyses. *Syst. Biol.* 64, 608–620. <https://doi.org/10.1093/sysbio/syv015>.

Spoor, F., Leakey, M.G., Gathogo, P.N., Brown, F.H., Anton, S.C., McDougall, I., Kiarie, C., Manthi, F.K., Leakey, L.N., 2007a. Implications of new early *Homo* fossils from Ileret, east of Lake Turkana, Kenya. *Nature* 448, 688–691. <https://doi.org/10.1038/nature05986>.

Spoor, F., Leakey, M.G., Gathogo, P.N., Brown, F.H., Antón, S.C., McDougall, I., Kiarie, C., Manthi, F.K., Leakey, L.N., 2007b. Implications of new early *Homo* fossils from Ileret, east of Lake Turkana, Kenya. *Nature* 448, 688–691. <https://doi.org/10.1038/nature05986>.

Strait, D.S., 2013. The biogeographic implications of early hominin phylogeny. In: Reed, K.E., Fleagle, J.G., Leakey, R.E. (Eds.), *The Paleobiology of *Australopithecus**. Springer, Dordrecht, pp. 183–191. [https://doi.org/10.1007/978-94-007-5919-0\\_12](https://doi.org/10.1007/978-94-007-5919-0_12).

Strait, D.S., Grine, F.E., 2004. Inferring hominoid and early hominid phylogeny using craniodental characters: The role of fossil taxa. *J. Hum. Evol.* 47, 399–452. <https://doi.org/10.1016/j.jhevol.2004.08.008>.

Strait, D.S., Grine, F.E., Moniz, M.A., 1997. A reappraisal of early hominid phylogeny. *J. Hum. Evol.* 32, 17–82. <https://doi.org/10.1006/jhev.1996.0097>.

Strait, D.S., Wood, B.A., 1999. Early hominid biogeography. *Proc. Natl. Acad. Sci. USA* 96, 9196–9200. <https://doi.org/10.1073/pnas.96.16.9196>.

Su, D.F., Harrison, T., 2008. Ecological implications of the relative rarity of fossil hominins at Laetoli. *J. Hum. Evol.* 55, 672–681. <https://doi.org/10.1016/j.jhevol.2008.07.003>.

Szumik, C.A., Goloboff, P.A., 2004. Areas of endemism: An improved optimality criterion. *Syst. Biol.* 53, 968–977. <https://doi.org/10.1080/10635150490888859>.

Thalmann, O., Fischer, A., Lankester, F., Pääbo, S., Vigilant, L., 2007. The complex evolutionary history of gorillas: Insights from genomic data. *Mol. Biol. Evol.* 24, 146–158. <https://doi.org/10.1093/molbev/msl160>.

Timmermann, A., Yun, K.-S., Raia, P., Ruan, J., Mondanaro, A., Zeller, E., Zollikofer, C., Ponce de León, M., Lemmon, D., Willeit, M., 2022. Climate effects on archaic human habitats and species successions. *Nature* 604, 495–501. <https://doi.org/10.1038/s41586-022-04600-9>.

Trauth, M.H., Maslin, M.A., Deino, A.L., Junginger, A., Lesoloyia, M., Odada, E.O., Olago, D.O., Olaka, L.A., Strecker, M.R., Tiedemann, R., 2010. Human evolution in a variable environment: The amplifier lakes of eastern Africa. *Quat. Sci. Rev.* 29, 2981–2988. <https://doi.org/10.1016/j.quascirev.2010.07.007>.

Turner, A., Wood, B., 1993. Taxonomic and geographic diversity in robust australopithecines and other African Plio-Pleistocene larger mammals. *J. Hum. Evol.* 24, 147–168. <https://doi.org/10.1006/jhev.1993.1011>.

Veldhuis, M.P., Ritchie, M.E., Ogutu, J.O., Morrison, T.A., Beale, C.M., Estes, A.B., Mwakilema, W., Ojwang, G.O., 2019. The Serengeti squeeze: Cross-boundary human impacts compromise an iconic protected ecosystem. *Science* 363, 1424–1428.

Vilhena, D.A., Antonelli, A., 2015. A network approach for identifying and delimiting biogeographical regions. *Nat. Commun.* 6, 6848. <https://doi.org/10.1038/ncomms7848>.

Villaseñor, A., Bobe, R., Behrensmeyer, A.K., 2020. Middle Pliocene hominin distribution patterns in eastern Africa. *J. Hum. Evol.* 147, 102856. <https://doi.org/10.1016/j.jhevol.2020.102856>.

VRba, E.S., 1992. Mammals as a key to evolutionary theory. *J. Mammal.* 73, 1–28. <https://doi.org/10.2307/1381862>.

Vuorio, V., Muchiru, A., Reid, R.S., Ogutu, J.O., 2014. How pastoralism changes savanna vegetation: Impact of old pastoral settlements on plant diversity and abundance in south-western Kenya. *Biodivers. Conserv.* 23, 3219–3240. <https://doi.org/10.1007/s10531-014-0777-4>.

Walker, A., Leakey, R.E., Harris, J.M., Brown, F.H., 1986. 2.5-myrr *Australopithecus boisei* from west of Lake Turkana, Kenya. *Nature* 322, 517–522. <https://doi.org/10.1038/322517a0>.

Webster, M.T., 2009. Patterns of autosomal divergence between the human and chimpanzee genomes support an allopatric model of speciation. *Gene* 443, 70–75. <https://doi.org/10.1016/j.gene.2009.05.006>.

Wells, J.C., Stock, J.T., 2007. The biology of the colonizing ape. *Am. J. Phys. Anthropol.* 134, 191–222. <https://doi.org/10.1002/ajpa.20735>.

White, T.D., WoldeGabriel, G., Asfaw, B., Ambrose, S., Beyene, Y., Bernor, R.L., Boisserie, J.-R., Currie, B., Gilbert, H., Haile-Selassie, Y., 2006. Asa Issie, Aramis and the origin of *Australopithecus*. *Nature* 440, 883–889. <https://doi.org/10.1038/nature04629>.

Won, Y.-J., Hey, J., 2005. Divergence population genetics of chimpanzees. *Mol. Biol. Evol.* 22, 297–307. <https://doi.org/10.1093/molbev/msi017>.

Wood, B., 1992. Early hominin species and speciation. *J. Hum. Evol.* 22, 351–365. [https://doi.org/10.1016/0047-2484\(92\)90065-H](https://doi.org/10.1016/0047-2484(92)90065-H).

Wood, B., Boyle, E.K., 2016. Hominin taxon diversity: Fact or fantasy? *Am. J. Phys. Anthropol.* 159, S37–S78. <https://doi.org/10.1002/ajpa.22902>.

Wood, B., Smith, R.J., 2022. Towards a more realistic interpretation of the human fossil record. *Quat. Sci. Rev.* 295, 107722. <https://doi.org/10.1016/j.quascirev.2022.107722>.

Wynn, J.G., Alemseged, Z., Bobe, R., Grine, F.E., Negash, E.W., Sponheimer, M., 2020. Isotopic evidence for the timing of the dietary shift toward C<sub>4</sub> foods in eastern African *Paranthropus*. *Proc. Natl. Acad. Sci. USA* 117, 21978–21984. [https://doi.org/10.1073/pnas.200622117](https://doi.org/10.1073/pnas.2006221117).